Geomechanics and Engineering, *Vol. 34, No. 3 (2023) 233-250*
https://doi.org/10.12989/gae.2023.34.3.233

A novel hyperbolic integral-Quasi-3D theory for flexural response of laminated composite plates

Ahmed Frih[1], Fouad Bourada*[2,3], Abdelhakim Kaci[2,4], Mohammed Bouremana[1], Abdelouahed Tounsi[2,5,6,7a], Mohammed A. Al-Osta[6,7], Khaled Mohamed Khedher[8] and Mohamed Abdelaziz Salem[9]

[1]*Laboratoire des Structures et Matériaux Avancés dans le Génie Civil et Travaux Publics, Faculté de Technologie, Département de Génie Civil, Université de Sidi Bel Abbes, Algeria*
[2]*Material and Hydrology Laboratory, University of Sidi Bel Abbes, Faculty of Technology, Civil Engineering Department, Algeria*
[3]*Science and Technology Department, Faculty of Science and Technology, Tissemsilt University, Algeria*
[4]*Université Dr Tahar Moulay, Faculté de Technologie, Département de Génie Civil et Hydraulique, BP 138 Cité En-Nasr 20000 Saida, Algérie*
[5]*YFL (Yonsei Frontier Lab), Yonsei University, Seoul, Korea*
[6]*Department of Civil and Environmental Engineering, King Fahd University of Petroleum & Minerals, 31261 Dhahran, Eastern Province, Saudi Arabia*
[7]*Interdisciplinary Research Center for Construction and Building Materials, KFUPM, 31261 Dhahran, Saudi Arabia*
[8]*Department of Civil Engineering, College of Engineering, King Khalid University, Abha 61421, Saudi Arabia*
[9]*Department of Industrial Engineering, College of Engineering, King Khalid University, Abha 61421, Saudi Arabia*

(*Received April 10, 2023, Revised June 17, 2023, Accepted June 19, 2023*)

Abstract. This paper investigates the flexural analysis of isotropic, transversely isotropic, and laminated composite plates using a new higher-order normal and shear deformation theory. In the present theory, only five unknown functions are involved compared to six or more unknowns used in the other similar theories. The developed theory does not need a shear correction factor. It can satisfy the zero traction boundary conditions on the top and the bottom surfaces of the plate as well as account for sufficient distribution of the transverse shear strains. The thickness stretching effect is considered in the computation. A simply supported was considered on all edges of the plate. The plate is subjected to uniform and sinusoidal distributed load in the static analysis. Laminated composite, isotropic, and transversely isotropic plates are considered. The governing equations are obtained utilizing the virtual work principle. The differential equations are solved via Navier's procedure. The results obtained from the developed theory are compared with other higher-order theories considered in the previous studies and 3D elasticity solutions. The results showed that the proposed theory accurately and effectively predicts the bidirectional bending responses of laminated composite plates. Several parametric studies are presented to illustrate the various parameters influencing the static response of the laminated composite plates.

Keywords: bidirectional bending; composite plate; isotropic; Navier's procedure; normal stress; novel quasi-3D theory; transversely isotropic

1. Introduction

Composite materials are now widely used in many fields, including aeronautics, naval, automotive, sports, and leisure. This is mainly due to the increasingly demanding needs of the industry. Lightness, rigidity, and resistance requirements make composites essential in all these sectors.

The key concept of composites is combining two or more materials with different characteristics, which do not have separated characteristics of value but form a material with essential properties. The fibers used as reinforcement have significantly better mechanical properties (strength and rigidity) than the same material in solid form: the reduction in the characteristic dimensions often implies an improvement in the mechanical performance because the fiber has, through the manufacturing process, a structure more perfect solid material and because the probability of finding significant defects decreases with the dimensions (Mouritz *et al.* 2001, Ye *et al.* 2005, Gibson 2016, Nikbakt *et al.* 2018). A composite laminate is a special orthotropic material. It can be modeled as a single surface with multiple layers of orthotropic materials. The material thus obtained is heterogeneous and anisotropic. The fibers give the mechanical resistance while the matrix binds the fibers, protects them, and transfers the loads to the fibers by shear.

In order to correctly predict the behavior of this kind of structure, several plate theories with different approaches have been developed to evaluate the response of laminated plates. These theories subdivide into three theories: the classical laminated plate theory (CLPT), the first order shear deformation theories (FSDT), and higher order shear deformation theories (HSDT). A general review and

*Corresponding author, Professor
E-mail: bouradafouad@yahoo.fr
[a]Professor
E-mail: tou_abdel@yahoo.com

ISSN: 2005-307X (Print), 2092-6219 (Online)

assumptions of his theories on composite plates can be observed in (Noor 1973, Doğruoğlu and Omurtag 2000, Huang and Thambiratnam 2001, Ghugal and Shimpi 2001, Setoodeh and Karami 2004, Aguiar *et al.* 2012, Ozutok *et al.* 2014, Kar and Panda 2015, Kolahchi *et al.* 2016, Aldousari 2017, Soliman *et al.* 2018, Selmi and Bisharat 2018, Cuong-Le *et al.* 2019ab, Khatir *et al.* 2019, Zenzen et al.2020, Bochkareva and Lekomtsev 2022, Cho 2022a, Fan *et al.* 2022, Hagos *et al.* 2022, Huang *et al.* 2022, Liu *et al.* 2022, Man 2022, Wu and Fang 2022, Zhu *et al.* 2022). The simplest laminate theory is CLPT, based on the Kirchhoff hypothesis. It is only suitable for thin plates where the transverse shear deformation can be ignored. Ding *et al.* (2022) have employed the classical theory (Euler-Bernoulli) to analyze the nonlinear resonance of Halpin-Tsai of FG graphene platelet reinforced (FGGPLRC) beams using the modified Lindstedt-Poincare method. The nonlinear snap-buckling and resonance of the clamped-hinged and hinged-hinged FG-GPLRC curved beams in investigated by Gan and She (2023) based on the Euler-Bernoulli beam theory. It is not suitable to predict the response of the plate where the transverse shear deformation is more critical such as the moderately thick or thick plates (Zhang and Global 2001, Wang *et al.* 2016, Wang and Zu 2017). Several theoretical models capable of predicting the response of a laminated plate and considering the shear deformation have been developed to surmount this problem. The FSDT was developed and modified by (Reissner 1944, Reissner 1945, and Mindlin 1951). However, a suitable shear correction factor is needed. Gan *et al.* (2023) studied the wave propagation in the porous graphene platelets reinforced metal foams circular plates with the help of the first-order shear deformation theory. Based on the FSDT formulation and the Galerkin method, Li *et al.* (2023) examined the thermal post-buckling of graphene platelets strengthened metal foams plates. To incorporate the curvature effect of the normal after deformation, several theories known as HSDT have been developed, and the displacements can be considered quadratic or cubic across the thickness of the plate. A variationally consistent higher-order theory is needed to account for the shear deformation. It satisfies the conditions on the top and bottom faces of the plate of zero transverse shear stress. It does not need correction factors proposed for plate analysis (Kar *et al.* 2015, Ghasemabadian and Kadkhodayan 2016, Sobhy and Zenkour 2018, Zenkour 2018, Madenci 2019, Vinyas 2020, Madenci and Özütok 2020, Navale and Pise 2021, Onyeka and Edozie 2021). Ding and She (2021) have adopted a novel high-order shear theory to examine the snap buckling of the FG curved pipes conveying fluid with considering the geometric nonlinearity and thermal effects. Chen *et al.* (2022) investigated the impact of the thermal environement on the nonlinear dynamic analysis of FG carbon nanotube reinforced fluid-conveying pipe based on the higher-order shear deformation theory. Based on the assumption of the third-order shear deformation theory, Zhang *et al.* (2023a) presented the wave propagations analysis in the doubly curved spherical- and cylindrical- panels in which the structures are reinforced by carbon nanotubes (CNTs).

It is important to note that the 2-D theories (i.e., CPT, FSDT, and HSDT) mentioned above do not take into account the effect of thickness stretching, considering a constant transverse displacement through the thickness, leading to theories of shear deformation that ignore stretching ($\varepsilon_z = 0$) . This assumption is incorrect, specifically for thick laminated plates. Higher order normal shear and strain theories that consider the effect of thickness stretching have been stated in the work of Carrera *et al.* 2011 using the unified formulation, which is substantial in thick plates. Therefore, it should be taken into consideration. To include the impact of the stretching ($\varepsilon_z \neq 0$), many quasi-3D theories with the combination of many shear deformation theories were developed in the literature to study the mechanical behaviors of thick plates (Matsunaga 2009, Thai and Kim 2013, Jha *et al.* 2013, Shahsavari *et al.* 2018, Fang and Bui 2019, Adhikari and Singh 2019). These theories are computationally heavy because they generate a large number of unknowns (Carrera *et al.* 2011 with fifteen unknowns, Talha and Singh 2010 with thirteen unknowns, Chen *et al.* 2009 and Reddy 2011 with eleven unknowns and Neves *et al.* 2012a, 2012b and 2013 with nine unknowns, Zenkour 2007, Adhikari and Singh 2018, Mantari and Guedes Soares 2012 and 2013 with six unknowns). On the other hand, thus, it is possible to develop a novel accurate theory of shear and higher-order normal strain that is quite simple to use and concurrently keeps essential physical characteristics.

Based on the literature, it is found that in recent years many researchers have paid attention to analyzing the laminated composite plates in the framework of the quasi-3D theory. For example, Mantari and Canales (2016) investigated a unified quasi-3D HSDT for the bending analysis of laminated cross-ply beams utilizing an unavailable unified HSDT for composite beams with the thickness stretching effect. Han *et al.* (2018) studied the response of free vibration and buckling of multilayered composite beams using the proposed refined four-unknown quasi-3D zigzag beam theory. The beams are subjected to axial mechanical loading and uniform temperature variation. Kharghani and Guedes Soares (2020) used various equivalent single-layer theories with shape functions of polynomial and trigonometric to investigate the buckling and post-buckling response of composite laminates and compared the obtained results with 3D finite element and experimental results. Doan *et al.* (2020) presented the stress concentration phenomenon at the points with structural jumping, force jumping, and unexpected changes in boundary conditions of laminated cylinder shells. Zenkour and El-Shahrany (2021) presented a Quasi-3D theory for the vibration and deflection of a multilayered composite plate based on simple and refined sinusoidal shear deformation plate theories where the visco-elastic foundations model simulates the interaction between the smart composite sandwich plate and the surrounding medium. Shao *et al.* (2021) developed a unified procedure to investigate the free and transient vibration behavior of a composite laminated beam exposed to general boundary conditions under a thermal scenario. The effect of axial–shear–flexural–stretching coupling with the thermal stress and the impact of Poisson's ratio is considered. Using the reverberation ray matrix method, the

mode shapes, natural frequencies, and transient responses of composite laminated beams are assessed. Also, others techniques are proposed. For exemples, She *et al*. (2022) have used the first order shear deformation theory and Hamiltonian variational principle to analyze the wave propagation of FG plate with considering the physical neutral surface concept. Xu and She (2022) analyzed thermal post-buckling behavior of imperfect FG pipes using the Euler-Lagrange principle and the two-step perturbation method. The thermal stability of the simply supported and clamped imperfect cylindrical shells is examined by Zhang *et al.* (2023b) based on Donnell nonlinear shell theory and Eulerian-Lagrange equations. The snap-buckling of the FG-CNTs nanotubes (CNTs) in thermal environment is investigated by Zhang *et al*. (2021) with considering the Chen-Yao's surface elastic theory, geometric nonlinearity and Euler-Lagrange equations.

This present study aims to develop a simple integral quasi-3D theory with just five unknown displacement functions against displacement functions with six or more unknowns utilized in the corresponding ones to analyze the bidirectional bending of laminated composite, isotropic, and transversely isotropic plates. The influence of both transverse shear and normal deformations is considered. The proposed model gives a parabolic distribution of the transverse shear stresses across the thickness direction and ensures the nullity at the upper and lower surfaces without using the shear correction factors. The governing equations are deduced from the virtual work principle and determined by the Navier method. Comparative studies are conducted to verify the accuracy and efficiency of the current theory.

The consideration of the stretching effect leads to a very good prediction of the flexural characteristics of the composites which ensures a correct pre-dimensioning of the plates which can be used in several sectors.

2. Theoretical formulation

The system to be considered is shown schematically in Fig. 1.

2.1 Kinematic relations and constitutive relations

In this article, the conventional HSDTs with thickness stretching effect are modified by proposing simplifying suppositions to reduce the number of unknowns number.

The displacement field of the existing HSDTs with thickness stretching effect is defined by

$$u(x,y,z)=u_0(x,y)-z\frac{\partial w_0}{\partial x}+f(z)\phi_x(x,y) \tag{1a}$$

$$v(x,y,z)=v_0(x,y)-z\frac{\partial w_0}{\partial y}+f(z)\phi_y(x,y) \tag{1b}$$

$$w(x,y,z)=w_0(x,y)+g(z)\phi_z(x,y) \tag{1c}$$

where: u_0 , v_0 , w_0 , φ_x , φ_y , and ϕ_z denote the six unknown displacements of the plate's mid-plane and $f(z)$ is the shape function defining the variation of stresses

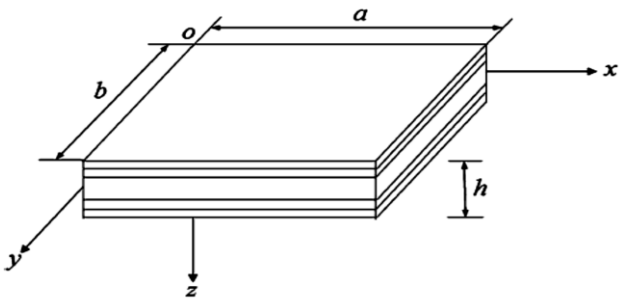

Fig. 1 Geometry and coordinates of the laminated plate

across the thickness and the transverse shear strains. With only five unknowns, in this article, a novel displacement field can be proposed as

$$u(x,y,z)=u_0(x,y)-z\frac{\partial w_0}{\partial x}+k_1\,f(z)\int\theta(x,y)\,dx \tag{2a}$$

$$v(x,y,z)=v_0(x,y)-z\frac{\partial w_0}{\partial y}+k_2\,f(z)\int\theta(x,y)\,dy \tag{2b}$$

$$w(x,y,z)=w_0(x,y)+g(z)\phi_z(x,y) \tag{2c}$$

k_1 and k_2 are the coefficients depend on the geometry. In this article, the $f(z)$ function is considered based on the hyperbolic as follows (Akavci and Tanrikulu 2008)

$$f(z)=-\left(\frac{3\pi}{2}z\,\mathrm{sech}^2\left(\frac{1}{2}\right)\right)+\frac{3\pi}{2}h\tanh\left(\frac{z}{h}\right)\ \text{and}\ g(z)=\frac{df(z)}{dz} \tag{3}$$

Among the advantages of the present theory, it takes into consideration both the normal and transverse shear deformations and it contains only five unknown variables compared to six or more in the others quasi-3D HSDTs which reduces the time and cost of calculation. The proposed model gives a parabolic distribution of the transverse shear stresses and ensures the boundary conditions in the top and bottom surfaces without requiring the shear correction factors.

The linear strain relations obtained from Eqs. (2(a)-2(c))of the displacement model can be used for the thin, moderately thick, and thick plates under consideration as follows

$$\begin{Bmatrix}\varepsilon_x\\ \varepsilon_y\\ \gamma_{xy}\end{Bmatrix}=\begin{Bmatrix}\varepsilon_x^0\\ \varepsilon_y^0\\ \gamma_{xy}^0\end{Bmatrix}+z\begin{Bmatrix}k_x^b\\ k_y^b\\ k_{xy}^b\end{Bmatrix}+f(z)\begin{Bmatrix}k_x^s\\ k_y^s\\ k_{xy}^s\end{Bmatrix},\qquad \begin{Bmatrix}\gamma_{yz}\\ \gamma_{xz}\end{Bmatrix}=g(z)\begin{Bmatrix}\gamma_{yz}^0\\ \gamma_{xz}^0\end{Bmatrix},\varepsilon_z=g'(z)\,\varepsilon_z^0 \tag{4}$$

Where:

$$\begin{Bmatrix}\varepsilon_x^0\\ \varepsilon_y^0\\ \gamma_{xy}^0\end{Bmatrix}=\begin{Bmatrix}\dfrac{\partial u_0}{\partial x}\\ \dfrac{\partial v_0}{\partial y}\\ \dfrac{\partial u_0}{\partial y}+\dfrac{\partial v_0}{\partial x}\end{Bmatrix},\quad \begin{Bmatrix}k_x^b\\ k_y^b\\ k_{xy}^b\end{Bmatrix}=\begin{Bmatrix}-\dfrac{\partial^2 w_0}{\partial x^2}\\ -\dfrac{\partial^2 w_0}{\partial y^2}\\ -2\dfrac{\partial^2 w_0}{\partial x\partial y}\end{Bmatrix}, \tag{5a}$$

$$\begin{Bmatrix} k_x^s \\ k_y^s \\ k_{xy}^s \end{Bmatrix} = \begin{Bmatrix} k_1\theta \\ k_2\theta \\ k_1\dfrac{\partial}{\partial y}\int\theta\,dx + k_2\dfrac{\partial}{\partial x}\int\theta\,dy \end{Bmatrix}, \quad \begin{Bmatrix} \gamma_{yz}^0 \\ \gamma_{xz}^0 \end{Bmatrix} = \begin{Bmatrix} k_2\int\theta\,dy + \dfrac{\partial\varphi_z}{\partial y} \\ k_1\int\theta\,dx + \dfrac{\partial\varphi_z}{\partial x} \end{Bmatrix}, \quad \varepsilon_z^0 = \varphi_z \tag{5b}$$

The integrals involved in the above equations should be solved by a Navier-type solution and shall be given as

$$\frac{\partial}{\partial y}\int\theta\,dx = A'\frac{\partial^2\theta}{\partial x\partial y}, \frac{\partial}{\partial x}\int\theta\,dy = B'\frac{\partial^2\theta}{\partial x\partial y}, \quad \int\theta\,dx = A'\frac{\partial\theta}{\partial x}, \int\theta\,dy = B'\frac{\partial\theta}{\partial y} \tag{6}$$

where A' and B' are the coefficients expressed according to the type of solution utilized. In this case, Navier is used. Therefore, A' and B' are expressed as follows

$$A' = -\frac{1}{\alpha^2}, \quad B' = -\frac{1}{\beta^2}, k_1 = \alpha^2, k_2 = \beta^2 \tag{7}$$

where α and β are defined in expression (22).

The stress-strain relations of laminate in the k^{th} orthotropic layer can be obtained as

$$\begin{Bmatrix} \sigma_x \\ \sigma_y \\ \sigma_z \end{Bmatrix}^{(k)} = \begin{bmatrix} \overline{Q}_{11} & \overline{Q}_{12} & \overline{Q}_{13} \\ \overline{Q}_{12} & \overline{Q}_{22} & \overline{Q}_{23} \\ \overline{Q}_{13} & \overline{Q}_{23} & \overline{Q}_{33} \end{bmatrix}^{(k)} \begin{Bmatrix} \varepsilon_x \\ \varepsilon_y \\ \varepsilon_z \end{Bmatrix}^{(k)} \text{ and } \begin{Bmatrix} \tau_{xy} \\ \tau_{yz} \\ \tau_{xz} \end{Bmatrix}^{(k)} = \begin{bmatrix} \overline{Q}_{66} & 0 & 0 \\ 0 & \overline{Q}_{44} & 0 \\ 0 & 0 & \overline{Q}_{55} \end{bmatrix}^{(k)} \begin{Bmatrix} \gamma_{xy} \\ \gamma_{yz} \\ \gamma_{xz} \end{Bmatrix}^{(k)} \tag{8}$$

$\bar{Q}_{ij}$ represents the transformed elastic coefficients. The transformed material constants are given as

$$\begin{aligned}
\overline{Q}_{11} &= Q_{11}\cos^4\theta + 2(Q_{12}+2Q_{66})\sin^2\theta\cos^2\theta + Q_{22}\sin^4\theta \\
\overline{Q}_{12} &= (Q_{11}+Q_{22}-4Q_{66})\sin^2\theta\cos^2\theta + Q_{12}(\sin^4\theta+\cos^4\theta) \\
\overline{Q}_{13} &= Q_{13}\cos^2\theta + Q_{23}\sin^2\theta \\
\overline{Q}_{22} &= Q_{11}\sin^4\theta + 2(Q_{12}+2Q_{66})\sin^2\theta\cos^2\theta + Q_{22}\cos^4\theta \\
\overline{Q}_{23} &= Q_{13}\sin^2\theta + Q_{23}\cos^2\theta \\
\overline{Q}_{33} &= Q_{33} \\
\overline{Q}_{66} &= (Q_{11}+Q_{22}-2Q_{12}-2Q_{66})\sin^2\theta\cos^2\theta \\
&\quad + Q_{66}(\sin^4\theta+\cos^4\theta) \\
\overline{Q}_{44} &= Q_{44}\cos^2\theta + Q_{55}\sin^2\theta \\
\overline{Q}_{55} &= Q_{55}\cos^2\theta + Q_{44}\sin^2\theta
\end{aligned} \tag{9}$$

where θ denotes the material axes' angle of each layer with the reference coordinate axes and Q_{ij} represents the plane stress-reduced stiffnesses and can be given as follows

$$Q_{11} = \frac{E_1(1-\nu_{23}\nu_{32})}{\Delta}; \quad Q_{12} = \frac{E_1(\nu_{21}+\nu_{31}\nu_{23})}{\Delta}; \quad Q_{13} = \frac{E_1(\nu_{31}+\nu_{21}\nu_{32})}{\Delta}; \tag{10a}$$

$$Q_{22} = \frac{E_2(1-\nu_{13}\nu_{31})}{\Delta}; \quad Q_{23} = \frac{E_2(\nu_{32}+\nu_{12}\nu_{31})}{\Delta}; \quad Q_{33} = \frac{E_3(1-\nu_{12}\nu_{21})}{\Delta}; \tag{10b}$$

$$Q_{66} = G_{12}; \quad Q_{55} = G_{13}; \quad Q_{44} = G_{23}; \tag{10c}$$

$$\Delta = 1-\nu_{12}\nu_{21}-\nu_{23}\nu_{32}-\nu_{31}\nu_{13}-2\nu_{21}\nu_{32}\nu_{13} \tag{10d}$$

in which E_1, E_2, E_3 are the Young's moduli in the x, y and z directions, respectively, G_{23}, G_{13}, G_{12} are the shear moduli and ν_{ij} are the Poisson's ratios for stressed in the *i* - direction when the transverse strain in *j* - direction. Young's moduli and Poisson's ratios are related as

$$\nu_{ij}E_j = \nu_{ji}E_i \qquad (i, j = 1,2,3) \tag{11}$$

2.2 Virtual work principle

The governing equations and boundary conditions of the new simple quasi-3D hyperbolic shear deformation theory are derived utilizing the virtual work principle (Hadji 2020, Fenjan 2020) and can be expressed in analytical form as

$$\delta U + \delta V = 0 \tag{12}$$

where δU denotes the virtual strain energy. δV is the external virtual work resulting from an external load applied to the plate. Substituting the appropriate energy expressions can be determined.

$$\sum_{k=1}^{N}\int_{h_k}^{h_{k+1}}\int_{\Omega}\begin{pmatrix}\sigma_x^k\delta\varepsilon_x + \sigma_y^k\delta\varepsilon_y + \sigma_z^k\delta\varepsilon_z \\ +\tau_{xy}^k\delta\gamma_{xy} + \tau_{yz}^k\delta\gamma_{yz} + \tau_{xz}^k\delta\gamma_{xz}\end{pmatrix}d\Omega dz - \int_{\Omega} q\delta w\,d\Omega = 0 \tag{13}$$

where Ω the top is surface. q represents the distributed transverse load.

Eq. (12) can be obtained by putting Eqs. (4) and (8) into Eq. (13) and integrating within the plate's thickness as follows

$$\int_{\Omega}\begin{bmatrix} N_x\delta\varepsilon_x^0 + N_y\delta\varepsilon_y^0 + N_z\delta\varepsilon_z^0 + N_{xy}\delta\gamma_{xy}^0 \\ +M_x^b\delta k_x^b + M_y^b\delta k_y^b + M_{xy}^b\delta k_{xy}^b + M_x^s\delta k_x^s \\ +M_y^s\delta k_y^s + M_{xy}^s\delta k_{xy}^s + S_{yz}^s\delta\gamma_{yz}^s + S_{xz}^s\delta\gamma_{xz}^s - q\delta w\end{bmatrix}d\Omega = 0 \tag{14}$$

where the stress resultants *N*, *M*, and *S* can be given by

$$\left(N_i, M_i^b, M_i^s\right) = \sum_{k=1}^{N}\int_{h_k}^{h_{k+1}}(1, z, f)\sigma_i^k dz, \ (i = x, y, xy)$$
$$\left(S_{xz}^s, S_{yz}^s\right) = \sum_{k=1}^{N}\int_{h_k}^{h_{k+1}} g(z)\left(\tau_{xz}, \tau_{yz}\right)^k dz \text{ and } N_z = \sum_{k=1}^{N}\int_{h_k}^{h_{k+1}} g'(z)\sigma_z^k dz \tag{15}$$

where h_k and h_{k+1} are the top and bottom z-coordinates of the nth layer.

The stress resultants are obtained in terms of generalized displacements ($u_0, v_0, w_0, \theta, \varphi_z$) by putting Eq. (4) into Eq. (8) and the following results into Eq. (15) as follows

$$\begin{Bmatrix} N_x \\ N_y \\ N_{xy} \\ M_x^b \\ M_y^b \\ M_{xy}^b \\ M_x^s \\ M_y^s \\ M_{xy}^s \\ N_z \end{Bmatrix} = \begin{bmatrix} A_{11} & A_{12} & 0 & B_{11} & B_{12} & 0 & B_{11}^s & B_{12}^s & 0 & X_{13} \\ A_{12} & A_{22} & 0 & B_{12} & B_{22} & 0 & B_{12}^s & B_{22}^s & 0 & X_{23} \\ 0 & 0 & A_{66} & 0 & 0 & B_{66} & 0 & 0 & B_{66}^s & 0 \\ B_{11} & B_{12} & 0 & D_{11} & D_{12} & 0 & D_{11}^s & D_{12}^s & 0 & Y_{13} \\ B_{12} & B_{22} & 0 & D_{12} & D_{22} & 0 & D_{12}^s & D_{22}^s & 0 & Y_{23} \\ 0 & 0 & B_{66} & 0 & 0 & D_{11} & 0 & 0 & D_{66}^s & 0 \\ B_{11}^s & B_{12}^s & 0 & D_{11}^s & D_{12}^s & 0 & H_{11}^s & H_{12}^s & 0 & Y_{13}^s \\ B_{12}^s & B_{22}^s & 0 & D_{12}^s & D_{22}^s & 0 & H_{12}^s & H_{22}^s & 0 & Y_{23}^s \\ 0 & 0 & B_{66}^s & 0 & 0 & D_{66}^s & 0 & 0 & H_{66}^s & 0 \\ X_{13} & X_{23} & 0 & Y_{13} & Y_{23} & 0 & Y_{13}^s & Y_{23}^s & 0 & Z_{33} \end{bmatrix} \begin{Bmatrix} \frac{\partial u_0}{\partial x} \\ \frac{\partial v_0}{\partial y} \\ \frac{\partial u_0}{\partial y} + \frac{\partial v_0}{\partial x} \\ -\frac{\partial^2 w_0}{\partial x^2} \\ -\frac{\partial^2 w_0}{\partial y^2} \\ -2\frac{\partial^2 w_0}{\partial x\, \partial y} \\ k_1\theta \\ k_2\theta \\ (k_1A'+k_2B')\frac{\partial^2\theta}{\partial x\, \partial y} \\ \phi_z \end{Bmatrix} \tag{16a}$$

$$\begin{Bmatrix} S_{yz}^s \\ S_{xz}^s \end{Bmatrix} = \begin{bmatrix} A_{44}^s & 0 \\ 0 & A_{55}^s \end{bmatrix} \begin{Bmatrix} k_2B'\dfrac{\partial\theta}{\partial y} + \dfrac{\partial\varphi_z}{\partial y} \\ k_1A'\dfrac{\partial\theta}{\partial x} + \dfrac{\partial\varphi_z}{\partial x} \end{Bmatrix} \tag{16b}$$

where

$$\left(A_{ij}, A_{ij}^s, B_{ij}, D_{ij}, B_{ij}^s, D_{ij}^s, H_{ij}^s\right) = \sum_{k=1}^{N}\int_{h_{k-1}}^{h_k} Q_{ij}^k \left(1, g^2(z), z, z^2, f(z), z\,f(z), f^2(z)\right)dz \tag{17a}$$

$$\left(X_{ij}, Y_{ij}, Y_{ij}^s, Z_{ij}\right) = \sum_{k=1}^{N}\int_{h_{k-1}}^{h_k} \left(1, z, f(z), g'(z)\right) g'(z) Q_{ij}^k dz \tag{17b}$$

2.3 Plate governing equations

By employing the generalized displacement–strain expressions (Eqs. (4) and (5)) and stress-strain expressions (Eq. (8)), and applying the integration by parts and the fundamental lemma of variational calculus and gathering the coefficients of δu_0, δv_0, δw_0, $\delta\theta$ and $\delta\varphi_z$ in Eq. (14), the governing equations are determined as

$$\begin{aligned}
&\delta u_0: && \frac{\partial N_x}{\partial x} + \frac{\partial N_{xy}}{\partial y} = 0 \\
&\delta v_0: && \frac{\partial N_{xy}}{\partial x} + \frac{\partial N_y}{\partial y} = 0 \\
&\delta w_0: && \frac{\partial^2 M_x^b}{\partial x^2} + 2\frac{\partial^2 M_{xy}^b}{\partial x\,\partial y} + \frac{\partial^2 M_y^b}{\partial y^2} + q = 0 \\
&\delta\theta: && -k_1 M_x^s - k_2 M_y^s - (k_1A'+k_2B')\frac{\partial^2 M_{xy}^s}{\partial x\,\partial y} \\
& && + k_1A'\frac{\partial S_{xz}^s}{\partial x} + k_2B'\frac{\partial S_{yz}^s}{\partial y} = 0 \\
&\delta\phi_z: && -N_z + \frac{\partial S_{xz}^s}{\partial x} + \frac{\partial S_{yz}^s}{\partial y} = 0
\end{aligned} \tag{18}$$

Putting Eq. (16) into Eq. (18), the governing equations of the present quasi-3D hyperbolic shear deformation theory can be obtained in terms of displacements (u_0, v_0, w_0, θ, φ_z) as

$$\begin{aligned}
&A_{11}d_{11}u_0 + A_{66}d_{22}u_0 + (A_{12}+A_{66})d_{12}v_0 + X_{13}d_1\phi_z \\
&-B_{11}d_{111}w_0 - (B_{12}+2B_{66})d_{122}w_0 \\
&+\left(B_{66}^s(k_1A'+k_2B')\right)d_{122}\theta + \left(B_{11}^s k_1 + B_{12}^s k_2\right)d_1\theta = 0
\end{aligned} \tag{19a}$$

$$\begin{aligned}
&A_{22}d_{22}v_0 + A_{66}d_{11}v_0 + (A_{12}+A_{66})d_{12}u_0 + X_{23}d_2\phi_z \\
&-B_{22}d_{222}w_0 - (B_{12}+2B_{66})d_{112}w_0 \\
&+\left(B_{66}^s(k_1A'+k_2B')\right)d_{112}\theta + \left(B_{22}^s k_2 + B_{12}^s k_1\right)d_2\theta = 0
\end{aligned} \tag{19b}$$

$$\begin{aligned}
&B_{11}d_{111}u_0 + (B_{12}+2B_{66})d_{122}u_0 + (B_{12}+2B_{66})d_{112}v_0 \\
&+B_{22}d_{222}v_0 + Y_{13}d_{11}\phi_z + Y_{23}d_{22}\phi_z - D_{11}d_{1111}w_0 \\
&-2(D_{12}+2D_{66})d_{1122}w_0 - D_{22}d_{2222}w_0 + \left(D_{11}^s k_1 + D_{12}^s k_2\right)d_{11}\theta \\
&+2\left(D_{66}^s(k_1A'+k_2B')\right)d_{1122}\theta + \left(D_{12}^s k_1 + D_{22}^s k_2\right)d_{22}\theta + q = 0
\end{aligned} \tag{19c}$$

$$\begin{aligned}
&-\left(B_{11}^s k_1 + B_{12}^s k_2\right)d_1u_0 - \left(B_{66}^s(k_1A'+k_2B')\right)d_{122}u_0 \\
&-\left(B_{66}^s(k_1A'+k_2B')\right)d_{112}v_0 - \left(B_{12}^s k_1 + B_{22}^s k_2\right)d_2v_0 \\
&-k_1Y_{13}^s\phi_z - k_2Y_{23}^s\phi_z + \left(D_{11}^s k_1 + D_{12}^s k_2\right)d_{11}w_0 \\
&+2\left(D_{66}^s(k_1A'+k_2B')\right)d_{1122}w_0 + \left(D_{12}^s k_1 + D_{22}^s k_2\right)d_{22}w_0 \\
&-H_{11}^s k_1^2\,\theta - H_{22}^s k_2^2\,\theta - 2H_{12}^s k_1 k_2\theta \\
&-\left((k_1A'+k_2B')^2 H_{66}^s\right)d_{1122}\theta + A_{44}^s(k_2B')^2 d_{22}\theta \\
&+A_{55}^s(k_1A')^2 d_{11}\theta + A_{44}^s(k_2B')d_{22}\phi_z + A_{55}^s(k_1A')d_{11}\phi_z = 0
\end{aligned} \tag{19d}$$

$$\begin{aligned}
&-X_{13}d_1u_0 - X_{23}d_2v_0 - Z_{33}\phi_z + Y_{13}d_{11}w_0 + Y_{23}d_{22}w_0 \\
&+(A_{44}^s - Y_{23}^s)(k_2B')d_{22}\theta + (A_{55}^s - Y_{13}^s)(k_1A')d_{11}\theta \\
&+A_{44}^s d_{22}\phi_z + A_{55}^s d_{11}\phi_z = 0
\end{aligned} \tag{19e}$$

where d_{ij}, d_{ijl} and d_{ijlm} denote the differential operators

$$d_{ij} = \frac{\partial^2}{\partial x_i\partial x_j},\quad d_{ijl} = \frac{\partial^3}{\partial x_i\partial x_j\partial x_l},\quad d_{ijlm} = \frac{\partial^4}{\partial x_i\partial x_j\partial x_l\partial x_m},\quad d_i = \frac{\partial}{\partial x_i},\quad (i,j,l,m=1,2). \tag{20}$$

3. Solution procedure

In the present work, the structure is assumed to be simply supported in the four opposite edges. By employing Navier's method, the following Fourier series can be obtained in which the solution of the displacement variables (u_0, v_0, w_0, θ, φ_z) can satisfy automatically the simply supported boundary conditions

$$\begin{Bmatrix} u_0 \\ v_0 \\ w_0 \\ \theta \\ \varphi_z \end{Bmatrix} = \sum_{n=1,3,5}^{n=\infty}\sum_{m=1,3,5}^{m=\infty} \begin{Bmatrix} U_{mn}\cos(\alpha x)\sin(\beta y) \\ V_{mn}\sin(\alpha x)\cos(\beta y) \\ W_{mn}\sin(\alpha x)\sin(\beta y) \\ X_{mn}\sin(\alpha x)\sin(\beta y) \\ \Phi_{mn}\sin(\alpha x)\sin(\beta y) \end{Bmatrix} \tag{21}$$

where (U_{mn}, V_{mn}, W_{mn}, X_{mn}, Φ_{mn}) are unknown functions to be calculated.

with

$$\alpha = m\pi / a\,,\ \beta = n\pi / b \tag{22}$$

q is the transverse load that can be expanded as

$$q(x,y) = \sum_{m=1}^{\infty}\sum_{n=1}^{\infty} Q_{mn} \sin \alpha x \sin \beta y \tag{23}$$

where

$$Q_{mn} = \frac{4}{ab}\int_0^a \int_0^b q(x,y)\sin \alpha x \sin \beta y dx dy = \begin{cases} q_0 & \text{for sinusoidal ly distribute d load,} \\ \dfrac{16q_0}{mn\pi^2} & \text{for uniformaly distribute d load} \end{cases} \tag{24}$$

The analytical solutions are determined from the following equations by putting Eqs. (21) and (23) into Eq. (19)

$$\begin{bmatrix} K_{11} & K_{12} & K_{13} & K_{14} & K_{15} \\ K_{12} & K_{22} & K_{23} & K_{24} & K_{25} \\ K_{13} & K_{23} & K_{33} & K_{34} & K_{35} \\ K_{14} & K_{24} & K_{34} & K_{44} & K_{45} \\ K_{15} & K_{25} & K_{35} & K_{45} & K_{55} \end{bmatrix} \begin{Bmatrix} U_{mn} \\ V_{mn} \\ W_{mn} \\ X_{mn} \\ \Phi_{mn} \end{Bmatrix} = \begin{Bmatrix} 0 \\ 0 \\ Q_{mn} \\ 0 \\ 0 \end{Bmatrix} \tag{25}$$

where

$$K_{11} = \alpha^2 B_{11} + \beta^2 A_{66},\ K_{12} = \alpha\beta(A_{12} + A_{66})$$
$$K_{13} = -\alpha^3 B_{11} - \alpha\beta^2 (B_{12} + 2B_{66})$$
$$K_{14} = -\alpha(k_1 B_{11}^s + k_2 B_{12}^s) + \alpha\beta^2 B_{66}^s (k_1 A' + k_2 B')$$
$$K_{15} = -\alpha X_{13},\ K_{22} = \alpha^2 A_{66} + \beta^2 A_{22}$$
$$K_{23} = -\alpha^2\beta(B_{12} + 2B_{66}) - \beta^3 B_{22}$$
$$K_{24} = -\beta(k_1 B_{12}^s + k_2 B_{22}^s) + \alpha^2\beta(k_1 A' + k_2 B') B_{66}^s$$
$$K_{25} = -\beta X_{23}$$
$$K_{33} = \alpha^4 D_{11} + \beta^4 D_{22} + 2\alpha^2\beta^2 (D_{12} + 2D_{66})$$
$$K_{34} = \alpha^2 k_1 D_{11}^s + (k_2\alpha^2 + k_1\beta^2) D_{12}^s + \beta^2 k_2 D_{22}^s - 2\alpha^2\beta^2 (k_1 A' + k_2 B') D_{66}^s$$
$$K_{35} = \alpha^2 Y_{13} + \beta^2 Y_{23}$$
$$K_{44} = k_1^2 H_{11}^s + k_2^2 H_{22}^s + 2k_1 k_2 H_{12}^s + \alpha^2\beta^2 (k_1 A' + k_2 B')^2 H_{66}^s + \alpha^2 (k_1 A')^2 A_{55}^s + \beta^2 (k_2 B')^2 A_{44}^s$$
$$K_{45} = k_1 Y_{13}^s + k_2 Y_{23}^s + \alpha^2 k_1 A' A_{55}^s + \beta^2 k_2 B' A_{44}^s$$
$$K_{55} = \alpha^2 A_{55}^s + \beta^2 A_{44}^s + Z_{33} \tag{26}$$

Solving Eq. (25), the unknowns U_{mn}, V_{mn}, W_{mn}, X_{mn}, Φ_{mn} can be obtained. By using Eqs. (1)-(8), all plate displacements and stress components can be calculated after determining the values of these unknown coefficients.

$$u(x,y,z) = (U_{mn} - z\alpha W_{mn} + k_1 A' \alpha\, f(z) X_{mn}) \cos(\alpha x) \sin(\beta y) \tag{27}$$

$$v(x,y,z) = (V_{mn} - z\beta W_{mn} + k_2 B' \beta\, f(z) X_{mn}) \sin(\alpha x) \cos(\beta y) \tag{28}$$

$$w(x,y,z) = (W_{mn} + g(z)\Phi_{mn}) \sin(\alpha x) \sin(\beta y) \tag{29}$$

$$\sigma_x^k = \left\{ \begin{array}{l} \bar{Q}_{11}^k \left(-\alpha U_{mn} + z\alpha^2 W_{mn} + k_1 f(z) X_{mn}\right) + \\ \bar{Q}_{12}^k \left(-\alpha U_{mn} + z\beta^2 V_{mn} + f(z) k_2 X_{mn}\right) \\ + \bar{Q}_{13}^k g'(z) \Phi_{mn} \end{array} \right\} \sin(\alpha x) \sin(\beta y) \tag{30}$$

$$\sigma_y^k = \left\{ \begin{array}{l} \bar{Q}_{12}^k \left(-\alpha U_{mn} + z\alpha^2 W_{mn} + k_1 f(z) X_{mn}\right) + \\ \bar{Q}_{22}^k \left(-\alpha U_{mn} + z\beta^2 V_{mn} + f(z) k_2 X_{mn}\right) \\ + \bar{Q}_{23}^k g'(z) \Phi_{mn} \end{array} \right\} \sin(\alpha x) \sin(\beta y) \tag{31}$$

$$\tau_{xy}^k = \bar{Q}_{66}^k \left\{ \beta U_{mn} + \alpha V_{mn} - 2\left(\frac{z}{h}\right) h\alpha\beta W_{mn} + (k_1 A' + k_2 B')\alpha\beta\, f(z) X_{mn} \right\} \cos(\alpha x) \cos(\beta y) \tag{32}$$

The transverse shear stresses are obtained by using constitutive relations and giving a discontinuity of transverse shear stresses at the layer interface. The equations for transverse shear stresses are written as

$$\left(\tau_{xz}^k\right)^{CR} = \bar{Q}_{55}^k \alpha\, g(z) (k_1 A' X_{mn} + \Phi_{mn}) \cos(\alpha x) \sin(\beta y) \tag{33}$$

$$\left(\tau_{yz}^k\right)^{CR} = \bar{Q}_{44}^k \beta\, g(z) (k_2 B' X_{mn} + \Phi_{mn}) \sin(\alpha x) \cos(\beta y) \tag{34}$$

The continuity of the shear stresses at the layer interface can be determined by obtaining the equations for transverse shear stresses through the equilibrium equations from the theory of elasticity as follows

$$\frac{\partial \sigma_x}{\partial x} + \frac{\partial \tau_{xy}}{\partial y} + \frac{\partial \tau_{xz}}{\partial z} = 0;\ \frac{\partial \sigma_y}{\partial y} + \frac{\partial \tau_{xy}}{\partial x} + \frac{\partial \tau_{xz}}{\partial z} = 0 \tag{35}$$

The relations in the case of in-plane normal and shear stresses $(\sigma_x, \sigma_y, \tau_{xy})$ in Eq. (35) are used for individual layers. Transverse shear stresses that are determined utilizing the constitutive relations are specified by $\tau_{xz}^{CR}, \tau_{yz}^{CR}$. However, the transverse shear stresses that are determined using the equilibrium equations are indicated by $\tau_{xz}^{EE}, \tau_{yz}^{EE}$.

The material properties of the plate that are used to obtain numerical results are given below

Isotropic

$$E_1 = E_2 = E_3 = 210GPa,$$
$$G_{13} = G_{23} = G_{12} = G = \frac{E}{2(1+\nu)},\qquad \nu_{12} = \nu_{32} = \nu_{31} = \nu = 0.3 \tag{36}$$

Transversely isotropic

$$E_1 = E_2 = 0.04,\quad E_3 = 0.5,\ G_{13} = G_{23} = 0.06,\ G_{12} = 0.016,\qquad \nu_{12} = \nu_{32} = \nu_{31} = 0.25 \tag{37}$$

Laminated composite (graphite-epoxy)

$$\frac{E_1}{E_2} = 25,\quad \frac{E_3}{E_2} = 1,\quad \frac{G_{12}}{E_2} = \frac{G_{13}}{E_2} = 0.5,\quad \frac{G_{23}}{E_2} = 0.2,\qquad \nu_{12} = \nu_{13} = \nu_{23} = 0.25 \tag{38}$$

Table 1 Comparison of nondimensional displacements and stresses for isotropic square plate (b = a)

S	Theory	Model	$\bar{u}$ $(h/2)$	$\bar{w}$ (0)	$\bar{\sigma}_x$ $(h/2)$	$\bar{\sigma}_y$ $(h/2)$	$\bar{\tau}_{xy}$ $(-h/2)$	$\bar{\tau}_{zx}^{CR}$ (0)	$\bar{\tau}_{zx}^{EE}$ (0)	$\bar{\tau}_{yz}^{CR}$ (0)	$\bar{\tau}_{yz}^{EE}$ (0)
						SDL					
	Present	I-HySDT	0,044	3,6588	0,2237	0,2237	0,1063	0,2426	0,2333	0,2426	0,2333
4	Pagano (1969)	Exact	0.0454	3.6630	0.2040	0.2040	–	0.2361	–	0.2□61	–
	Sayyad and Ghugal (2014)	SSNDT	0.0440	3.6534	0.2267	0.2267	0.1063	0.2444	0.2355	0.2444	0.2355
	Present	I-HySDT	0,0439	2,938	0,2087	0,2087	0,1062	0,2435	0,2364	0,2435	0,2364
10	Pagano (1969)	Exact	0.0443	2.9425	0.1988	0.1988	–	0.2383	–	0.2383	–
	Sayyad and Ghugal (2014)	SSNDT	0.0440	3.6534	0.2267	0.2267	0.1063	0.2444	0.2355	0.2444	0.2355
	Present	I-HySDT	0,044	2,8332	0,2066	0,2066	0,1062	0,2437	0,2368	0,2437	0,2368
20	Pagano (1969)	Exact	0.0440	2.8377	0.1979	0.1979	–	0.2386	–	0.2386	–
	Sayyad and Ghugal (2014)	SSNDT	0.0439	2.8286	0.2105	0.2105	0.1060	0.2455	0.2384	0.2455	0.2384
	Present	I-HySDT	0,044	2,8038	0,206	0,206	0,1062	0,2437	0,2369	0,2437	0,2369
50	Pagano (1969)	Exact	0.0440	2.8082	0.1976	0.1976	–	0.2386	–	0.2386	–
	Sayyad and Ghugal (2014)	SSNDT	0.0439	2.7991	0.2100	0.2100	0.1060	0.2456	0.2385	0.2456	0.2385
	Present	I-HySDT	0,044	2,7996	0,206	0,206	0,1062	0,2437	0,237	0,2437	0,237
100	Pagano (1969)	Exact	0.0440	2.8040	0.1976	0.1976	–	0.2387	–	0.2387	–
	Sayyad and Ghugal (2014)	SSNDT	0.0439	2.7949	0.2099	0.2099	0.1060	0.2456	0.2385	0.2456	0.2385
						UDL					
	Present	I-HySDT	0,0742	5,688	0,3166	0,3166	0,2099	0,4802	0,3911	0,4802	0,3911
4	Pagano (1969)	Exact	0.0758	5.6947	0.2948	0.2948	–	0.4606	–	0.4606	–
	Sayyad and Ghugal (2014)	SSNDT	0.0742	5.6799	0.3185	0.3185	0.2082	0.4833	0.4201	0.4833	0.4201
	Present	I-HySDT	0,0735	4.6326	0,3022	0,3022	0,1969	0,5023	0,4623	0,5023	0,4623
10	Pagano (1969)	Exact	0.0741	4.6397	0.2886	0.2886	–	0.4871	–	0.4871	–
	Sayyad and Ghugal (2014)	SSNDT	0.0734	4.6252	0.3071	0.3071	0.1954	0.5044	0.4814	0.5044	0.4814
	Present	I-HySDT	0.0735	4.4800	0.3002	0.3002	0.1951	0.5096	0.4858	0.5096	0.4858
20	Pagano (1969)	Exact	0.0737	4.4871	0.2876	0.2876	–	0.4931	–	0.4931	–
	Sayyad and Ghugal (2014)	SSNDT	0.0734	4.4727	0.3054	0.3054	0.1942	0.5083	0.4921	0.5083	0.4921
	Present	I-HySDT	0,0735	4,4372	0,2996	0,2996	0,1946	0,5133	0,4977	0,5133	0,4977
50	Pagano (1969)	Exact	0.0736	4.4442	0.2874	0.2874	–	0.4946	–	0.4946	–
	Sayyad and Ghugal (2014)	SSNDT	0.0734	4.4299	0.3050	0.3050	0.1941	0.5091	0.4942	0.5091	0.4942
	Present	I-HySDT	0,0735	4,4311	0,2996	0,2996	0,1946	0,5138	0,4993	0,5138	0,4993
100	Pagano (1969)	Exact	0.0736	4.4381	0.2873	0.2873	–	0.4949	–	0.4949	–
	Sayyad and Ghugal (2014)	SSNDT	0.0734	4.4238	0.3049	0.3049	0.1941	0.5092	0.4944	0.5092	0.4944

4. Numerical results and discussions

The present simple integral quasi-3D shear deformation theory with only 5 unknowns is applied to several static bending examples. At this stage, numerical examples are given in order to validate the present theory's accuracy and efficiency.

The following nondimensional equations can be employed

$$\bar{u} = \frac{E_3}{qhS^3} u\left(0, \frac{b}{2}, \frac{z}{h}\right), \quad \bar{w} = \frac{100E_3}{qhS^4} w\left(\frac{a}{2}, \frac{b}{2}, \frac{z}{h}\right),$$
$$\bar{\sigma}_x = \frac{h^2}{qS^2}\sigma_x\left(\frac{a}{2}, \frac{b}{2}, \frac{z}{h}\right), \quad \bar{\sigma}_y = \frac{h^2}{qS^2}\sigma_y\left(\frac{a}{2}, \frac{b}{2}, \frac{z}{h}\right),$$
$$\bar{\tau}_{xy} = \frac{1}{qS^2}\tau_{xy}\left(\frac{a}{2}, \frac{b}{2}, \frac{z}{h}\right), \quad \bar{\tau}_{xz} = \frac{1}{qS}\tau_{xz}\left(0, \frac{b}{2}, \frac{z}{h}\right), \tag{39}$$
$$\bar{\tau}_{yz} = \frac{1}{qS}\tau_{yz}\left(0, \frac{b}{2}, \frac{z}{h}\right)$$

where S = a/h and E_3 denote the elastic modulus of the middle layer.

4.1 Bidirectional bending analysis

4.1.1 Isotropic plates

The first numerical example illustrates a square isotropic plate subjected to sinusoidal and uniform distributed load.

The results of stresses and transversal displacement determined by the present quasi-3D shear model with only 5 unknowns are compared to those obtained for bending by the exact solution carried out by Pagano (1969) and quasi-3D solutions reported by Sayyad and Ghugal (2014), as presented in Table 1. The agreeability between the present and published results can be observed. However, the present model is found to be overestimated the obtained values of transverse shear stress when utilizing constitutive relations. Whereas the calculated values of transverse shear stress using the equilibrium equations of the theory of elasticity of Pagano, 1969 are accurate.

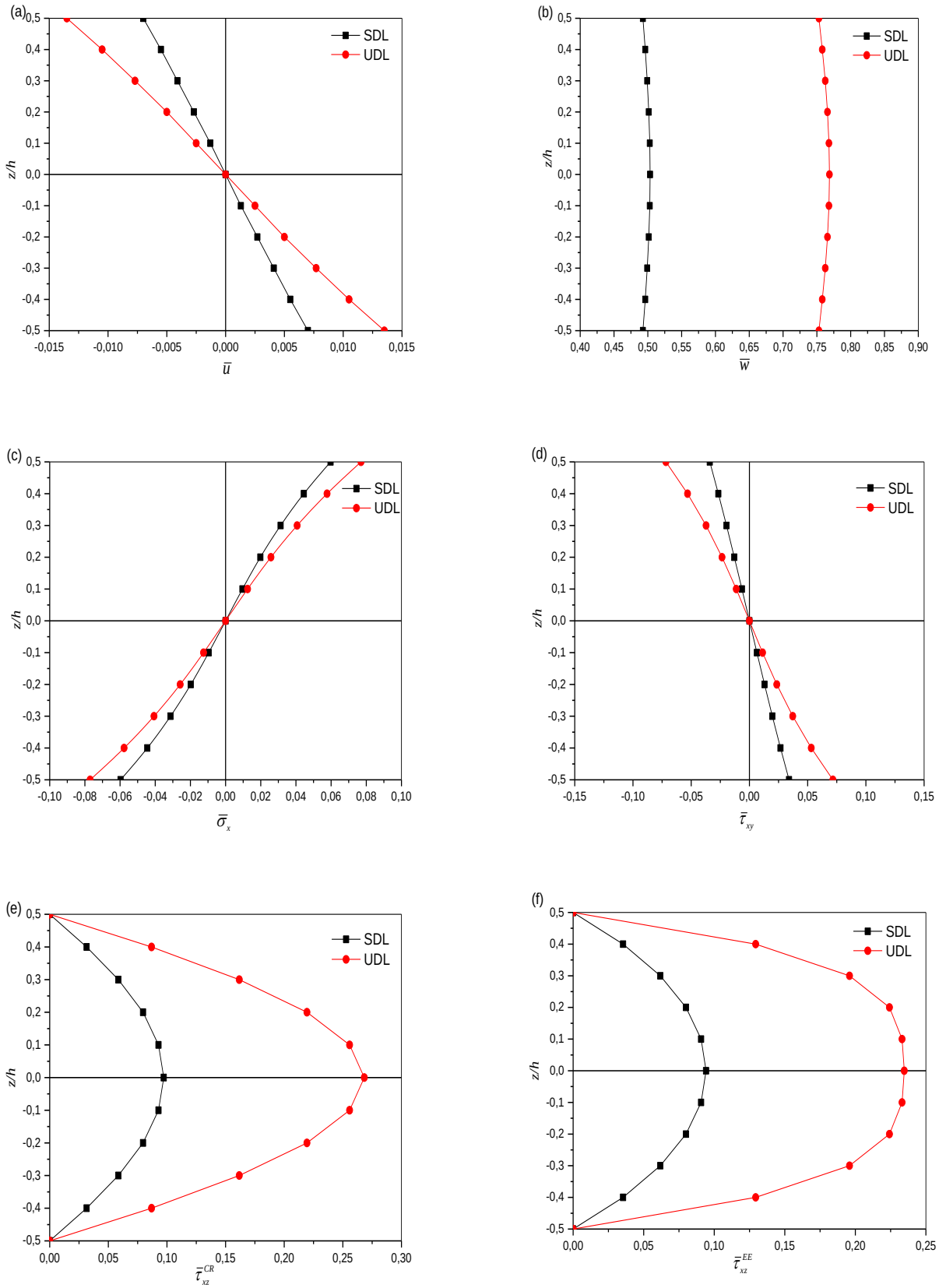

Fig. 2 Variation of nondimensional displacement and stresses through the thickness of rectangular isotropic plate (a=2b) subjected to SDL/UDL with (S = 10): (a) the axial displacement$\bar{u}$, (b) the deflection $\bar{w}$,(c) the axial stress $\bar{\sigma}_x$, (d) the in-plane shear stress$\bar{\tau}_{xy}$, (e) the transverse shear stress $\bar{\tau}_{xz}^{CR}$ and (e) the transversal shear stress $\bar{\tau}_{xz}^{EE}$

Table 2 Comparison of nondimensional displacements and stresses for transversely isotropic square plate (b=a)

S	Theory	Model	$\bar{u}$ $(-h/2)$	$\bar{w}$ (0)	$\bar{\sigma}_x$ $(-h/2)$	$\bar{\sigma}_y$ $(-h/2)$	$\bar{\tau}_{xy}$ $(-h/2)$	$\bar{\tau}_{zx}^{CR}$ (0)	$\bar{\tau}_{zx}^{EE}$ (0)	$\bar{\tau}_{yz}^{CR}$ (0)	$\bar{\tau}_{yz}^{EE}$ (0)
						SDL					
4	Present	I-HySDT	0,5735	39,1503	0,1934	0,1934	0,1153	0,2439	0,2378	0,2439	0,2378
	Kirchhoff	CLPT	0.5669	36.091	0.1900	0.1900	0.1140	–	0.2387	–	0.2387
	Mindlin (1951)	FSDT	0.5669	39.257	0.1900	0.1900	0.1140	0.1592	0.2387	0.1592	0.2387
	Reddy (1984)	HSDT	0.5705	38.952	0.1937	0.1937	0.1147	0.2385	0.2379	0.2385	0.2379
	Sayyad and Ghugal (2014)	SSNDT	0.5736	39.146	0.1936	0.1936	0.1153	0.2461	0.2377	0.2461	0.2377
10	Present	I-HySDT	0,5679	36,5812	0,1908	0,1908	0,1142	0,2442	0,2385	0,2442	0,2385
	Kirchhoff	CLPT	0.5669	36.091	0.1900	0.1900	0.1140	–	0.2387	–	0.2387
	Mindlin (1951)	FSDT	0.5669	36.598	0.1900	0.1900	0.1140	0.1592	0.2387	0.1592	0.2387
	Reddy (1984)	HSDT	0.5635	36.295	0.1914	0.1914	0.1133	0.2387	0.2386	0.2387	0.2386
	Sayyad and Ghugal (2014)	SSNDT	0.5679	36.578	0.1909	0.1909	0.1142	0.2463	0.2385	0.2463	0.2385
						UDL					
4	Present	I-HySDT	0,9629	61,5829	0,2798	0,2798	0,2199	0,4992	0,4522	0,4992	0,4522
	Kirchhoff	CLPT	0.9479	57.127	0.2763	0.2763	0.2086	–	0.4950	–	0.4950
	Mindlin (1951)	FSDT	0.9479	61.732	0.2763	0.2763	0.2086	0.3300	0.4950	0.3300	0.4950
	Reddy (1984)	HSDT	0.9570	61.250	0.2806	0.2806	0.2178	0.4912	0.4816	0.4912	0.4816
	Sayyad and Ghugal (2014)	SSNDT	0.9629	61.577	0.2803	0.2803	0.2180	0.5024	0.4686	0.5024	0.4686
10	Present	I-HySDT	0,9502	57,8391	0,2772	0,2772	0,2107	0,5105	0,4887	0,5105	0,4887
	Kirchhoff	CLPT	0.9479	57.127	0.2763	0.2763	0.2086	–	0.4950	–	0.4950
	Mindlin (1951)	FSDT	0.9479	57.864	0.2763	0.2763	0.2086	0.3300	0.4950	0.3300	0.4950
	Reddy (1984)	HSDT	0.9427	57.385	0.2782	0.2782	0.2136	0.4944	0.4927	0.4944	0.4927
	Sayyad and Ghugal (2014)	SSNDT	0.9500	57.835	0.2775	0.2775	0.2098	0.5098	0.4917	0.5098	0.4917

The through-thickness variations of displacements and stresses for isotropic plate ($a = 2b$) subjected to sinusoidal and uniform distributed load according to present higher-order normal and shear deformation theory are illustrated in figure 2 for aspect ratio 10. It can be seen from Fig. 2(a) and Fig. 2(b) that the axial displacement $\bar{u}$ and transverse displacement $\bar{w}$ under uniform distributed load are greater than those subject to a sinusoidal load. Fig. 2(c) shows the variation of axial stress $\bar{\sigma}_x$ across the thickness.

The stress is tensile and compressive at the plate's top and bottom surfaces, respectively. In Fig. 2(d), the in-plane shear stress $\bar{\tau}_{xy}$ is tensile and compressive at the bottom and the top surfaces, respectively.

For aspect ratio 10, the obtained nondimensional transverse shear stress $\bar{\tau}_{xz}^{CR}$ utilizing constitutive relation is shown in Fig. 2(e). It can be observed that the values of transverse shear stress satisfy the stress-free boundary conditions on plate's top and bottom surfaces. It should be noted that the values of $\bar{\tau}_{xz}$ obtained using the constitutive relations indicated by $\bar{\tau}_{xz}^{CR}$. The transverse shear obtained using constitutive relation under uniform distributed load is greater than that corresponding subject to a sinusoidal load. In Fig. 2(f), it can be observed that the nondimensional values of the transverse shear stress $\bar{\tau}_{xz}^{EE}$ at layer interface and calculated using equilibrium equations satisfy the continuity, where parabolic distribution and traction-free boundary conditions of shear stress are noted.

4.1.2 Transversely isotropic plates

The second example is performed for transversely isotropic square plates subjected to sinusoidal and uniform distributed load. This enhanced plate theory considers the effect of stretching and provides more accurate results that are very close to 3-D elasticity ones. Table 2 shows the calculated results of nondimensional displacement and stress. Results are compared with the CLPT of Kirchhoff, the FSDT of Mindlin (1951), and those from Reddy's shear deformation theory (Reddy 1984), considering $\varepsilon_z = 0$, and those from Sayyad and Ghugal (2014), accounting for ε_z. The results from the present quasi-3D higher-order plate theory taking into account $\varepsilon_z \neq 0$ are found to be in good agreement with those reported by Sayyad and Ghugal (2014), who as well consider $\varepsilon_z \neq 0$.

The nondimensional displacements and stresses through-thickness of the transversely isotropic rectangular plate (a=2b) subjected to SDL/UDL according to the present higher-order normal and shear deformation theory are illustrated in Fig. 3 for aspect ratio 10. It can be observed from Figs. 3(a) and 3(b) that the axial displacement $\bar{u}$ and transverse displacement $\bar{w}$ under uniform distributed load is greater than those subject to a sinusoidal load. Fig. 3(c) shows the variation of axial stress $\bar{\sigma}_x$ across the thickness. The stress is tensile and compressive at the plate's top and bottom surfaces. In Fig. 3(d), the in-plane shear stress $\bar{\tau}_{xy}$ is tensile and compressive

Table 3 Comparison of nondimensional displacements and stresses for two layers (0°/90°) anti-symmetric composite square plate (b = a)

S	Theory	Model	$\bar{u}$ $(-h/2)$	$\bar{w}$ (0)	$\bar{\sigma}_x$ $(-h/2)$	$\bar{\sigma}_y$ $(-h/2)$	$\bar{\tau}_{xy}$ $(-h/2)$	$\bar{\tau}_{zx}^{CR}$ (0)	$\bar{\tau}_{zx}^{EE}$ (0)	$\bar{\tau}_{yz}^{CR}$ (0)	$\bar{\tau}_{yz}^{EE}$ (0)
						SDL					
4	Present	I-HySDT	0,0111	1,9494	0,9039	0,0965	0,0562	0,127	0,1121	0,127	0,1121
	Zenkour (2007)	Exact	–	2.0670	0.8410	0.1090	0.0591	0.120	–	0.135	–
	Kirchhoff	CLPT	0.0088	1.0636	0.7157	0.0843	0.0525	–	0.122	–	0.122
	Mindlin (1951)	FSDT	0.0088	1.9682	0.7157	0.0843	0.0525	0.091	0.122	0.091	0.122
	Reddy (1984)	HSDT	0.0113	1.9985	0.9060	0.0891	0.0577	0.125	0.110	0.125	0.110
	Sayyad and Ghugal (2014)	SSNDT	0.0111	1.9424	0.9062	0.0964	0.0562	0.127	0.112	0.127	0.112
10	Present	I-HySDT	0,0092	1,21	0,7463	0,0872	0,053	0,1297	0,1202	0,1297	0,1202
	Zenkour (2007)	Exact	–	1.2250	0.7302	0.0886	0.0535	0.121	–	0.125	–
	Kirchhoff	CLPT	0.0088	1.0636	0.7157	0.0843	0.0525	–	0.122	–	0.122
	Mindlin (1951)	FSDT	0.0088	1.2083	0.7157	0.0843	0.0525	0.091	0.122	0.091	0.122
	Reddy (1984)	HSDT	0.0092	1.2161	0.7468	0.0851	0.0533	0.127	0.120	0.127	0.120
	Sayyad and Ghugal (2014)	SSNDT	0.0092	1.2089	0.7471	0.0876	0.0530	0.130	0.120	0.130	0.120
						UDL					
4	Present	I-HySDT	0,019	3,0098	1,2655	0,14	0,1074	0,2352	0,1315	0,2352	0,1315
	Zenkour (2007)	Exact	–	3.1580	1.1840	0.1590	–	0.246	–	0.279	–
	Kirchhoff	CLPT	0.0147	1.6955	1.0763	0.1269	0.0934	–	0.246	–	0.246
	Mindlin (1951)	FSDT	0.0144	3.0082	1.0636	0.1258	0.0992	0.191	0.239	0.191	0.239
	Reddy (1984)	HSDT	0.0190	3.0706	1.2691	0.1314	0.1070	0.241	0.143	0.241	0.143
	Sayyad and Ghugal (2014)	SSNDT	0.0189	2.9983	1.2603	0.1394	0.1104	0.239	0.136	0.239	0.136
10	Present	I-HySDT	0,0154	1,9096	1,108	0,1304	0,0963	0,2583	0,2047	0,2583	0,2047
	Zenkour (2007)	Exact	–	1.9320	1.0860	0.1300	–	0.246	–	0.248	–
	Kirchhoff	CLPT	0.0147	1.6955	1.0763	0.1269	0.0934	–	0.246	–	0.246
	Mindlin (1951)	FSDT	0.0146	1.9050	1.0533	0.1265	0.0961	0.194	0.244	0.194	0.244
	Reddy (1984)	HSDT	0.0154	1.9173	1.1049	0.1274	0.0977	0.264	0.214	0.264	0.214
	Sayyad and Ghugal (2014)	SSNDT	0.0153	1.9070	1.1057	0.1307	0.0978	0.266	0.210	0.266	0.210

at the plate's top and bottom surfaces, respectively, of the transversely isotropic rectangular plate (a=2b). For aspect ratio 10, the obtained nondimensional transverse shear stress $\bar{\tau}_{xz}^{CR}$ using constitutive relation is shown in Fig. 3(e). It can be observed that the values of transverse shear stress satisfy the stress-free boundary conditions on the plate's top and bottom surfaces. It should be noted that the values of $\bar{\tau}_{xz}$ obtained using the constitutive relations indicated by $\bar{\tau}_{xz}^{CR}$. The transverse shear obtained using constitutive relation under uniform distributed load is greater than that corresponding subject to a sinusoidal load. In Fig. 3(f), it can be observed that the nondimensional values of the transverse shear stress $\bar{\tau}_{xz}^{EE}$ at layer interface and calculated using equilibrium equations satisfy the continuity, where parabolic distribution and traction-free boundary conditions of shear stress are noted.

4.1.3 Cross-ply laminated composite plates

In the third example, the nondimensional displacement and stresses of the two layers (0°/90°) anti-symmetric cross-ply square and rectangular plates subjected to sinusoidal and uniform distributed load are illustrated in Tables 3 and 4. The present results are compared with the results of a sinusoidal shear and normal deformation theory (SSNDT) presented by Sayyad and Ghugal (2014), the exact 3D of Zenkour (2007), and CLPT of Kirchhoff, the FSDT of Mindlin (1951), and those from Reddy's shear deformation theory (Reddy 1984) where the effect of thickness stretching is neglected ($\varepsilon_z = 0$). The dimensionless displacement and stresses estimated by the new quasi-3D integral hyperbolic shear deformation theory with only 5 unknowns are almost identical to those evaluated by the SSNDT reported by Sayyad and Ghugal (2014) and the exact 3D solution of Zenkour (2007). Results are also compared with the CLPT of Kirchhoff, the FSDT of Mindlin (1951), and those from Reddy's shear deformation theory (Reddy 1984), considering $\varepsilon_z = 0$. It can be seen that the present theory (I-HySDT) and Reddy (1984) predict lower values of transverse shear stresses. In contrast, the theory of CLPT and Mindlin (1951) predicts excellent values of those calculated utilizing equilibrium equations. It can also be seen that for a square plate, the transverse shear stresses $\bar{\tau}_{xz}$ and $\bar{\tau}_{yz}$ are identical.

The nondimensional values of displacements and stresses through-thickness of two layers (0°/90°) anti-symmetric rectangular plate $(a = 2b)$ subjected to

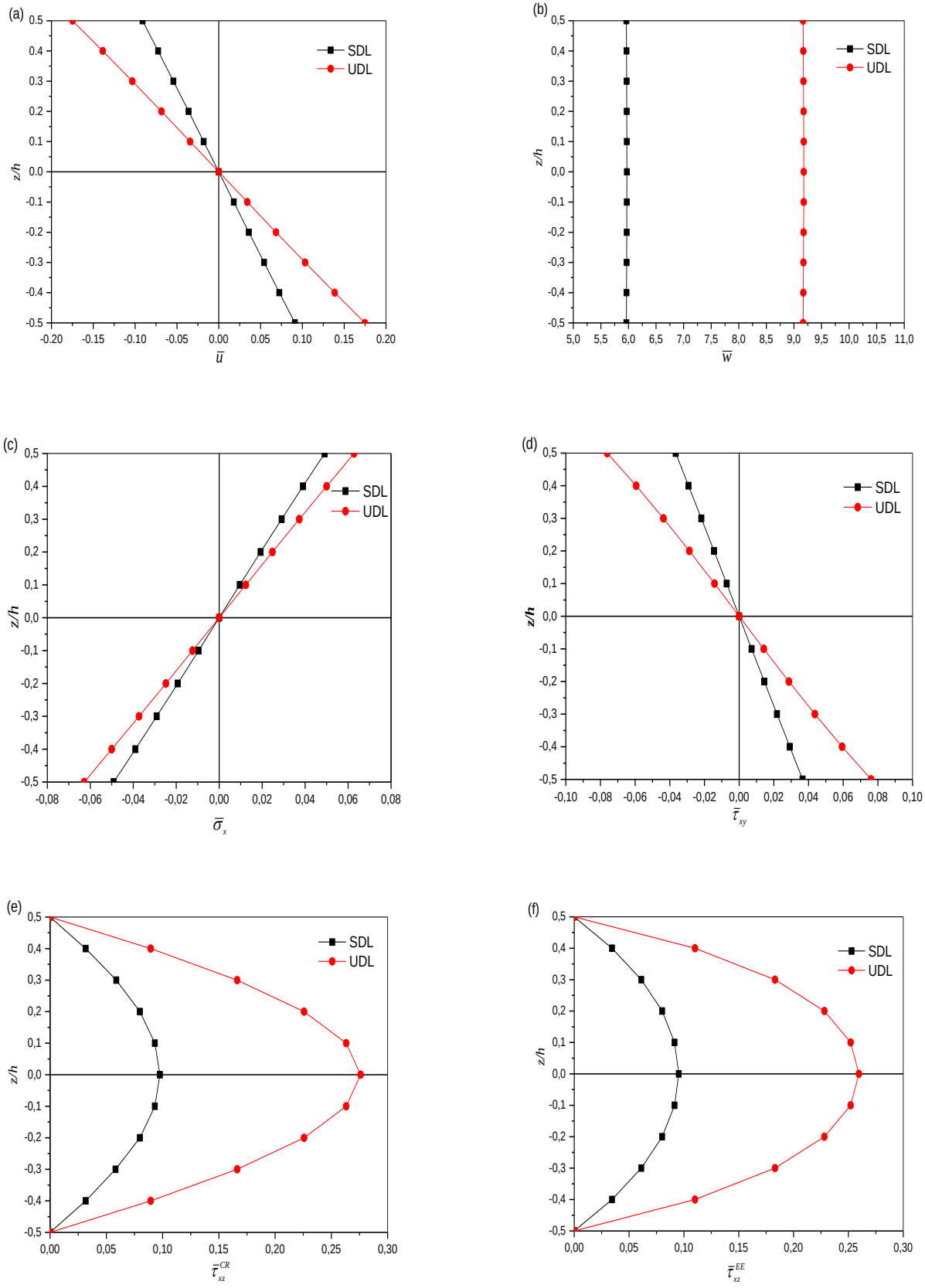

Fig. 3 Variation of nondimensional displacement and stresses through the thickness of the transversely isotropic rectangular plate (a=2b) subjected to SDL/UDL with (S = 10): (a) the axial displacement$\bar{u}$, (b) the deflection $\bar{w}$, (c) the axial stress $\bar{\sigma}_x$, (d) the in-plane shear stress$\bar{\tau}_{xy}$, (e) the transverse shear stress $\bar{\tau}_{xz}^{CR}$ and (e) the transversal shear stress $\bar{\tau}_{xz}^{EE}$

Table 4 Comparison of nondimensional displacements and stresses for two layers (0°/90 °) anti-symmetric composite rectangular plate (b = 3a)

S	Theory	Model	$\bar{u}$ $(-h/2)$	$\bar{w}$ (0)	$\bar{\sigma}_x$ $(h/2)$	$\bar{\sigma}_y$ $(h/2)$	$\bar{\tau}_{xy}$ $(-h/2)$	$\bar{\tau}_{zx}^{CR}$ (0)	$\bar{\tau}_{zx}^{EE}$ (0)	$\bar{\tau}_{yz}^{CR}$ (0)	$\bar{\tau}_{yz}^{EE}$ (0)
						SDL					
4	Present	I-HySDT	0,0246	4,0376	0,1922	0,2524	0,0438	0,2273	0,0237	0,2273	0,1956
	Zenkour (2007)	Exact	0.0220	4.3931	0.2246	0.3306	0.0598	0.2217	–	0.0527	–
	Kirchhoff	CLPT	0.0208	2.4628	0.1799	0.1918	0.0417	–	0.1942	–	0.0415
	Mindlin (1951)	FSDT	0.0204	4.1518	0.1780	0.3035	0.0447	0.1730	0.1923	0.0266	0.0556
	Reddy (1984)	HSDT	0.0248	4.1767	0.1825	0.3105	0.0589	0.2366	0.1759	0.0366	0.0513
	Sayyad and Ghugal (2014)	SSNDT	0.0246	4.0813	0.1904	0.3152	0.0530	0.2411	0.1799	0.0376	0.0511
10	Present	I-HySDT	0,0213	2,7073	0,1825	0,2146	0,0421	0,2312	0,0182	0,2312	0,2122
	Zenkour (2007)	Exact	0.0209	2.7760	0.1878	0.2277	0.0440	0.1995	–	0.0437	–
	Kirchhoff	CLPT	0.0208	2.4628	0.1799	0.1918	0.0417	–	0.1942	–	0.0415
	Mindlin (1951)	FSDT	0.0207	2.7346	0.1795	0.2250	0.0403	0.1748	0.1938	0.0213	0.0442
	Reddy (1984)	HSDT	0.0214	2.7430	0.1802	0.2252	0.0650	0.2426	0.1911	0.0307	0.0435
	Sayyad and Ghugal (2014)	SSNDT	0.0213	2.7161	0.1843	0.2257	0.0438	0.2480	0.1941	0.0310	0.0423
						UDL					
4	Present	I-HySDT	0,0362	5,5984	0,1516	0,1267	0,1267	0,3545	1,7476	0,3545	0,5676
	Zenkour (2007)	Exact	0.0319	6.1055	0.2985	0.2131	0.1450	0.3899	–	0.2196	–
	Kirchhoff	CLPT	0.0299	3.4757	0.2448	0.0594	0.1118	–	0.3148	–	0.2110
	Mindlin (1951)	FSDT	0.0295	5.7679	0.2432	0.2056	0.1367	0.2910	0.3151	0.1578	0.2246
	Reddy (1984)	HSDT	0.0364	5.7999	0.2477	0.1705	0.1466	0.3744	0.2118	0.2042	0.1599
	Sayyad and Ghugal (2014)	SSNDT	0.0362	5.6755	0.2566	0.1772	0.1435	0.3740	0.2077	0.2031	0.1545
10	Present	I-HySDT	0,0308	3,7995	0,8058	0,1178	0,1151	0,3806	0,0316	0,3806	2,5614
	Zenkour (2007)	Exact	0.0302	3.9030	0.2543	0.0860	0.1211	0.3478	–	0.2233	–
	Kirchhoff	CLPT	0.0299	3.4757	0.2448	0.0594	0.1118	–	0.3148	–	0.2110
	Mindlin (1951)	FSDT	0.0298	3.8452	0.2447	0.0862	0.1180	0.2925	0.3153	0.1536	0.2126
	Reddy (1984)	HSDT	0.0310	3.8554	0.2454	0.0802	0.1580	0.3973	0.2843	0.2129	0.1990
	Sayyad and Ghugal (2014)	SSNDT	0.0309	3.8152	0.2506	0.0803	0.1187	0.4033	0.2868	0.2162	0.1983

sinusoidal and uniform distributed load according to present higher-order normal and shear deformation theory are illustrated in Fig. 4 for aspect ratio 10.

It can be found from Figs. 4(a) and 4(b) that the axial displacement $\bar{u}$ and transverse displacement $\bar{w}$ under uniform distributed load is greater than those subject to a sinusoidal load. Fig. 4(c) displays the variation of axial stress $\bar{\sigma}_x$ across the thickness. It is clear that there is pronounced discontinuity at the layer interface. In Fig. 4(d), the in-plane shear stress $\bar{\tau}_{xy}$ is tensile and compressive at the plate's top and bottom surfaces, respectively, of a 2-layer (0°/90°) anti-symmetric rectangular plate.

For aspect ratio 10, the obtained nondimensional transverse shear stress $\bar{\tau}_{xz}^{CR}$ using constitutive relation is shown in Fig. 4(e).

It can be observed that the values of transverse shear stress satisfy the stress-free boundary conditions on the plate's top and bottom surfaces. It should be noted that the values of $\bar{\tau}_{xz}$ obtained using the constitutive relations indicated by $\bar{\tau}_{xz}^{CR}$

The transverse shear obtained using constitutive relation under uniform distributed load is greater than that corresponding subject to a sinusoidal load. In Fig. 4(f), it can be seen that the nondimensional values of the transverse shear stress $\bar{\tau}_{xz}^{EE}$ at layer interface and obtained using equilibrium equations satisfy the continuity, where parabolic distribution and traction-free boundary conditions of shear stress are noted.

5. Conclusions

A new higher-order shear and normal deformation theory is utilized to study the plates' bidirectional bending behavior. The theory includes stretching and shear deformation effects without using a shear correction factor. Furthermore, the governing equations and the number of unknowns are reduced to 5 compared to 6 or more unknowns used in the other theories.

The accuracy of the present theory is evaluated by comparing it with existing solutions. It was found that the results determined from the present theory have excellent

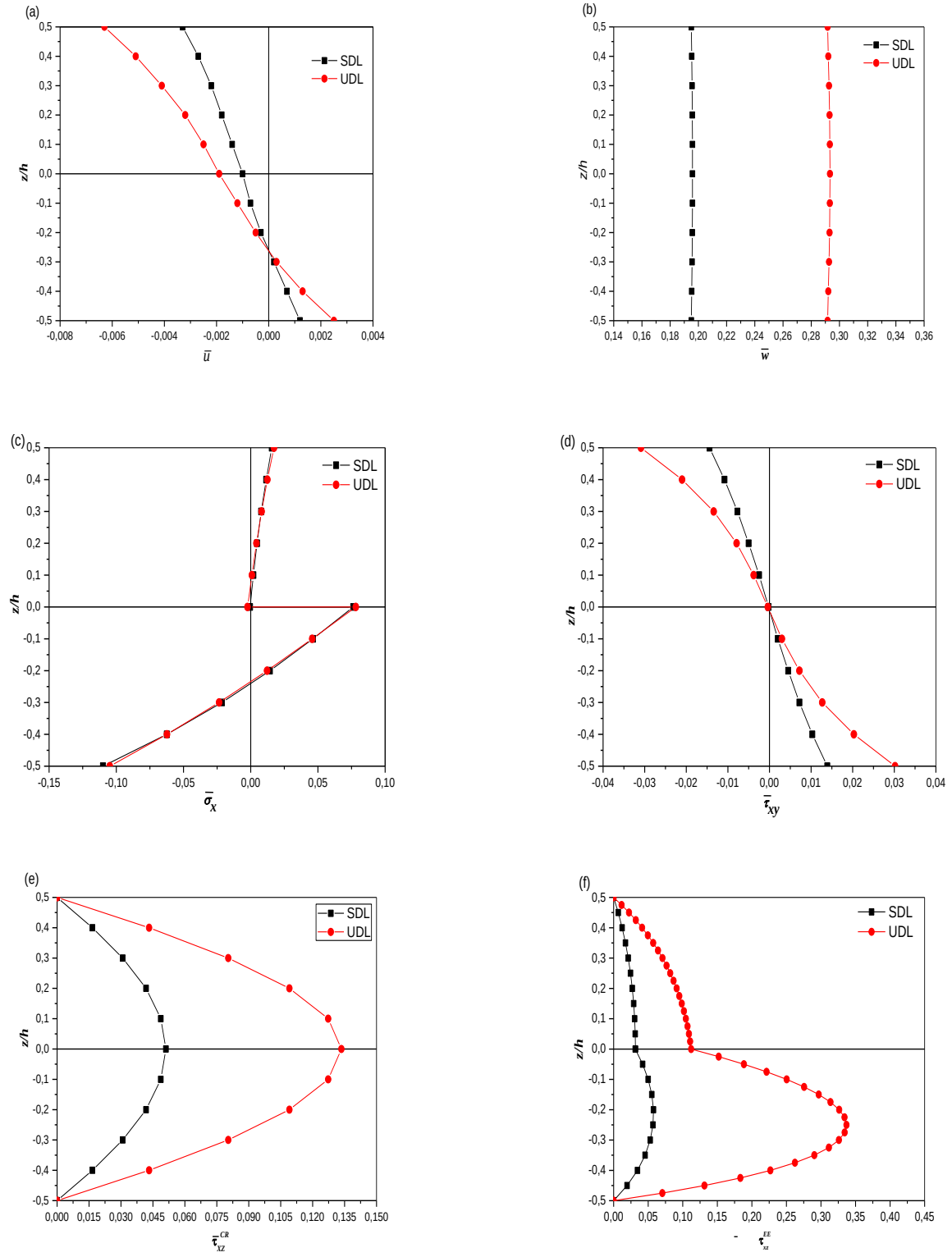

Fig. 4 Variation of non-dimensional displacement and stresses through the thickness of 2-layer (0°/90°) anti-symmetric rectangular plate (a=2b) subjected to SDL/UDL with (S = 10): (a) the axial displacement$\bar{u}$, (b) the deflection $\bar{w}$,(c)the axial stress $\bar{\sigma}_x$, (d) the in-plane shear stress$\bar{\tau}_{xy}$, (e) the transverse shear stress $\bar{\tau}_{xz}^{CR}$ and (e) the transversal shear stress $\bar{\tau}_{xz}^{EE}$

agreement with obtained results from the exact 3D solutions and the higher order shear deformation theory of Reddy for analyzing the bidirectional bending of laminated composite, isotropic, and transversely isotropic. It can be concluded that the present theory is simple and accurate in evaluating displacements and stresses of the bidirectional bending of

laminated composite, isotropic, and transversely isotropic.

An improvement of the proposed theory will be extended in the future investigations to consider other type of materials and structures with various scale and compared with experimental investigation (Akbas 2015, Avcar 2019, Ramteke *et al*. 2019, Ahmed *et al.* 2019, Rachedi *et al.* 2020, Yaylaci and Avcar 2020, Arefi and Zur 2020, Faleh 2020, Ramady *et al.* 2020, Cuong-Le *et al.* 2020ab, Khatir *et al.* 2021, Selmi 2020 and 2022, Yaylaci *et al.* 2021a, b, Madenci and Özkılıç 2021, Xiao *et al.* 2021, Alnujaie *et al.* 2021, Bashiri *et al.* 2021, Madenci 2021, Mansouri *et al.* 2021, Al-Toki *et al.* 2022, Hussain *et al.* 2022, Zhou *et al.* 2022, Cuong-Le *et al.* 2022a, b, Akbas 2022, Azandariani *et al.* 2022, Alimoradzadeh and Akbas 2022, Choi *et al.* 2022, Cho 2022b, Chinnapandi *et al.* 2022, Ding *et al.* 2022, Du *et al.* 2022, Mula *et al*. 2022, Rezaiee-Pajand *et al.* 2022, Tran and Cuong-Le 2022, Polat and Kaya 2022, Kumar and Kattimani 2022, Yaylaci *et al.* 2022c, Ghandourah *et al.* 2023, Zhang *et al*. 2023c, Zhang and She 2022, 2023, Madenci *et al.* 2023a,b, Ding and She 2023).

Acknowledgments

The Authors extend their appreciation to the Deanship Scientific Research at King Khalid University for funding this work through large group Research Project under grant number: **RGP2/422/44**.

References

Adhikari, B. andSingh, B.N. (2018), "An efficient higher order non-polynomial Quasi 3-D theory for dynamic responses of laminated composite plates", *Compos. Struct.*, **189**, 386-397. https://doi.org/10.1016/j.compstruct.2017.10.044.

Adhikari, B. and Singh, B.N. (2019), "Dynamic response of functionally graded plates resting on two-parameter-based elastic foundation model using a quasi-3D theory", *Mech. Based Des. Struct. Machines*. **47**(4), 399-429. https://doi.org/10.1080/15397734.2018.1555965.

Aguiar, R.M., Moleiro, F. and Soares, C.M. (2012), "Assessment of mixed and displacement-based models for static analysis of composite beams of different cross-sections", *Compos. Struct.*, **94**(2), 601-616. https://doi.org/10.1016/j.compstruct.2011.08.028.

Ahmed, R.A., Fenjan, R.M. and Faleh, N.M. (2019), "Analyzing post-buckling behavior of continuously graded FG nanobeams with geometrical imperfections", *Geomech. Eng.*, **17**(2), 175-180. https://doi.org/10.12989/gae.2019.17.2.175.

Akavci, S.S. and Tanrikulu, A.H. (2008), "Buckling and free vibration analyses of laminated composite plates by using two new hyperbolic shear-deformation theories", *Mech. Compos. Mater.*, **44**, 145-154. https://doi.org/10.1007/s11029-008-9004-2.

Akbas, S.D. (2015), "Wave propagation of a functionally graded beam in thermal environments", *Steel Compos. Struct.*, **19**(6), 1421-1447. https://doi.org/10.12989/scs.2015.19.6.1421.

Akbas, S.D. (2022), "Moving-load dynamic analysis of AFG beams under thermal effect", *Steel Compos. Struct.*, **42**(5), 649-655. https://doi.org/10.12989/scs.2022.42.5.649.

Aldousari, S.M. (2017), "Bending analysis of different material distributions of functionally graded beam", *Appl. Phys. A*, **123**(4), 1-9. https://doi.org/10.1007/s00339-017-0854-0.

Alimoradzadeh, M. and Akbas, S.D. (2022), "Nonlinear dynamic behavior of functionally graded beams resting on nonlinear viscoelastic foundation under moving mass in thermal environment", *Struct. Eng. Mech.*, **81**(6), 705-714. https://doi.org/10.12989/sem.2022.81.6.705.

Alnujaie, A., Akbas, Ş.D., Eltaher, M.A. and Assie, A. (2021), "Forced vibration of a functionally graded porous beam resting on viscoelastic foundation", *Geomech. Eng.*, **24**(1), 91-103. https://doi.org/10.12989/gae.2021.24.1.091.

Al-Toki, M.H.Z., Ali, H. A.K., Faleh, N.M. and Fenjan, R.M. (2022), "Numerical assessment of nonlocal dynamic stability of graded porous beams in thermal environment rested on elastic foundation", *Geomech. Eng.*, **28**(5), 455-461. https://doi.org/10.12989/gae.2022.28.5.455.

Arefi, M. and Zur, K.K. (2020), "Free vibration analysis of functionally graded cylindrical nanoshells resting on Pasternak foundation based on two-dimensional analysis", *Steel Compos. Struct*., **34**(4), 615-623. https://doi.org/10.12989/scs.2020.34.4.615.

Avcar, M. (2019), "Free vibration of imperfect sigmoid and power law functionally graded beams", *Steel Compos. Struct*., **30**(6), 603-615. https://doi.org/10.12989/scs.2019.30.6.603.

Azandariani, M.G., Gholami, M. and Nikzad, A. (2022), "Eringen's nonlocal theory for non-linear bending analysis of BGF Timoshenko nanobeams", *Adv. Nano Res*., **12**(1), 37-47. https://doi.org/10.12989/anr.2022.12.1.037.

Bashiri, A.H., Akbas, S.D., Abdelrahman, A.A., Assie, A., Eltaher, M.A. and Mohamed, E.F. (2021), "Vibration of multilayered functionally graded deep beams under thermal load", *Geomech. Eng.*, **24**(6), 545-557. https://doi.org/10.12989/gae.2021.24.6.545.

Bochkareva, S.A. and Lekomtsev, S.V. (2022), "Natural vibrations and hydroelastic stability of laminated composite circular cylindrical shells", *Struct. Eng. Mech.*, **81**(6), 769-780. https://doi.org/10.12989/sem.2022.81.6.769.

Carrera, E., Brischetto, S., Cinefra, M. and Soave, M. (2011), "Effects of thickness stretching in functionally graded plates and shells", *Compos. Part B: Eng.*, **42**(2), 123-133. https://doi.org/10.1016/j.compositesb.2010.10.005.

Chen, C.S., Hsu, C.Y. and Tzou, G.J. (2009), "Vibration and stability of functionally graded plates based on a higher-order deformation theory", *J. Reinforced Plast. Compos*., **28**(10), 1215-1234. https://doi.org/10.1177/0731684408088884.

Chen, X., Zhao, J.L., She, G.L., Jing, Y., Pu, H.Y. and Luo, J. (2022), "Nonlinear free vibration analysis of functionally graded carbon nanotube reinforced fluid-conveying pipe in thermal environment", *Steel Compos. Struct*., **45**(5), 641-652. https://doi.org/10.12989/scs.2022.45.5.641.

Chinnapandi, L.B.M., Pitchaimani, J. and Eltaher, M.A. (2022), "Vibro-acoustics of functionally graded porous beams subjected to thermo-mechanical loads", *Steel Compos. Struct.*, **44**(6), 829-843. https://doi.org/10.12989/scs.2022.44.6.829.

Cho, J.R. (2022b), "Thermal buckling analysis of metal-ceramic functionally graded plates by natural element method", *Struct. Eng. Mech.*, **84**(6), 723-731. https://doi.org/10.12989/sem.2022.84.6.723.

Cho, J.R. (2022a), "Nonlinear bending analysis of functionally graded CNT-reinforced composite plates", *Steel Compos. Struct.*, **42**(1), 23-32. https://doi.org/10.12989/scs.2022.42.1.023.

Choi, S.H., Heo, I., Kim, J.H., Jeong, H., Lee, J.Y. and Kim, K.S. (2022), "Flexural behavior of post-tensioned precast concrete girder at negative moment region", *Comput. Concrete*, **30**(1), 75-84. https://doi.org/10.12989/cac.2022.30.1.075.

Cuong-Le, T., Ferreira, A.J.M. and Abdel Wahab, M. (2019b), "A refined size-dependent couple stress theory for laminated composite micro-plates using isogeometric analysis", *Thin Wall.*

Struct., **145**, 106427. https://doi.org/10.1016/j.tws.2019.106427.

Cuong-Le, T., Nguyen, K.D., Nguyen-Trong, N., Khatir, S., Nguyen-Xuan, H. and Abdel-Wahab, M. (2020a), "A three-dimensional solution for free vibration and buckling of annular plate, conical, cylinder and cylindrical shell of FG porous-cellular materials using IGA", *Compos. Struct.*, **259**, 113216. https://doi.org/10.1016/j.compstruct.2020.113216.

Cuong-Le, T., Nguyen, K.D., Hoang-Le, M., Sang-To, T., Phan-Vu, P. and Abdel Wahab, M. (2022a), "Nonlocal strain gradient IGA numerical solution for static bending, free vibration and buckling of sigmoid FG sandwich nanoplate", *Physica B: Condensed Matter.*, **631**, 413726. https://doi.org/10.1016/j.physb.2022.413726.

Cuong-Le, T., Nguyen, K.D., Lee, J., Rabczuk, T. and Nguyen-Xuan, H. (2022b), "A 3D nano scale IGA for free vibration and buckling analyses of multi-directional FGM nanoshells", *Nanotechnology*, **33**(6), 065703. https://doi.org/10.1088/1361-6528/ac32f9.

Cuong-Le, T., Nguyen, T.N., Vu, T.H., Khatir, S. and Abdel Wahab, M. (2020b), "A geometrically nonlinear size-dependent hypothesis for porous functionally graded micro-plate", *Eng. with Comput.*, **38**(2022), 449-460. https://doi.org/10.1007/s00366-020-01154-0.

Cuong-Le, T., Tran, L.V., Vu-Huu, T. and Abdel-Wahab, M. (2019a), "The size-dependent thermal bending and buckling analyses of composite laminate microplate based on new modified couple stress theory and isogeometric analysis", *Comput. Method. Appl. M.*, **350**, 337-361. https://doi.org/10.1016/j.cma.2019.02.028.

Ding, F., Ding, H., He, C., Wang, L. and Lyu, F. (2022), "Method for flexural stiffness of steel-concrete composite beams based on stiffness combination coefficients", *Comput. Concrete*, **29**(3), 127-144. https://doi.org/10.12989/cac.2022.29.3.127.

Ding, H.X. and She, G.L. (2021), "A higher-order beam model for the snap-buckling analysis of FG pipes conveying fluid", *Struct. Eng. Mech.*, **80**(1), 63-72. https://doi.org/10.12989/sem.2021.80.1.063.

Ding, HX. and She, G.L. (2023), "Nonlinear resonance of axially moving graphene platelet-reinforced metal foam cylindrical shells with geometric imperfection", *Archiv. Civ. Mech. Eng.*, **23**, 97 (2023). https://doi.org/10.1007/s43452-023-00634-6.

Ding, H.X., Zhang, Y.W. and She, G.L. (2022), "On the resonance problems in FG-GPLRC beams with different boundary conditions resting on elastic foundations", *Comput. Concrete.*, **30**(6), 433-443. https://doi.org/10.12989/cac.2022.30.6.433.

Doan, T.N., Thanh, N.T., Van Chuong, P., Tho, N.C., Ta, N.T. and Nguyen, H.N. (2020), "Analysis of stress concentration phenomenon of cylinder laminated shells using higher-order shear deformation Quasi-3D theory", *Compos. Struct.*, **232**, 111526. https://doi.org/10.1016/j.compstruct.2019.111526.

Doğruoğlu, A.N. and Omurtag, M.H. (2000), "Stability analysis of composite-plate foundation interaction by mixed FEM", *J. Eng. Mech.*, **126**(9), 928-936. https://doi.org/10.1061/(ASCE)0733-9399(2000)126:9(928).

Du, M., Liu, J., Ye, W., Yang, F. and Lin, G. (2022), "A new semi-analytical approach for bending, buckling and free vibration analyses of power law functionally graded beams", *Struct. Eng. Mech.*, **81**(2), 179-194. https://doi.org/10.12989/sem.2022.81.2.179.

Faleh, N.M., Abboud, I.K. and Nori, A.F. (2020), "Nonlinear stability of smart nonlocal magneto-electro-thermo-elastic beams with geometric imperfection and piezoelectric phase effects", *Smart Struct. Syst.*, **25**(6), 707-717. https://doi.org/10.12989/sss.2020.25.6.707.

Fan, L., Kong, D., Song, J., Moradi, Z., Safa, M. and Khadimallah, M.A. (2022), "Optimization dynamic responses of laminated multiphase shell in thermo-electro-mechanical conditions", *Adv. Nano Res.*, **13**(1), 29-45. https://doi.org/10.12989/anr.2022.13.1.029.

Fang, W., Yu, T. and Bui, T.Q. (2019), "Analysis of thick porous beams by a quasi-3D theory and isogeometric analysis", *Compos. Struct.*, **221**, 110890. https://doi.org/10.1016/j.compstruct.2019.04.062.

Fenjan, R.M., Ahmed, R.A., Faleh, N.M. and Hani, F.M. (2020), "Static stability analysis of smart nonlocal thermo-piezo-magnetic plates via a quasi-3D formulation", *Smart Struct. Syst.*, **26**(1), 77-87. https://doi.org/10.12989/sss.2020.26.1.077.

Gan, L.L. and She, G.L. (2023), "Nonlinear snap-buckling and resonance of FG-GPLRC curved beams with different boundary conditions", *Geomech. Eng.*, **32**(5), 541-551. https://doi.org/10.12989/gae.2023.32.5.541.

Gan, L.L., Xu, J.Q. and She, G.L. (2023), "Wave propagation of graphene platelets reinforced metal foams circular plates", *Struct. Eng. Mech.*, **85**(5), 645-654. https://doi.org/10.12989/sem.2023.85.5.645.

Ghandourah, E., Hussain, M., Khadimallah, M.A., Alazwari, M., Ali, M.R. and Hefni, M.A. (2023), "Validity assessment of aspect ratios based on Timoshenko-beam model: Structural design", *Comput. Concrete.*, **31**(1), 1-7. https://doi.org/10.12989/cac.2023.31.1.001.

Ghasemabadian, M.A. and Kadkhodayan, M. (2016), "Investigation of buckling behavior of functionally graded piezoelectric (FGP) rectangular plates under open and closed circuit conditions", *Struct. Eng. Mech.*, **60**(2), 271-299. https://doi.org/10.12989/sem.2016.60.2.271.

Ghugal, Y.M. and Shimpi, R.P. (2001), "A review of refined shear deformation theories for isotropic and anisotropic laminated beams", *J. Reinf. Plast. Comp.*, **20**(3), 255-272. https://doi.org/10.1177/073168401772678283.

Gibson, R.F. (2016), "Principles of composite material mechanics", *CRC Press*. **20**(3). https://doi.org/10.1177/073168401772678283.

Hadji, L. (2020), "Influence of the distribution shape of porosity on the bending of FGM beam using a new higher order shear deformation model", *Smart Struct. Syst.*, **26**(2), 253-262. https://doi.org/10.12989/sss.2020.26.2.253.

Hagos, R.W., Choi, G., Sung, H. and Chang, S. (2022), "Substructuring-based dynamic reduction method for vibration analysis of periodic composite structures", *Compos. Mater. Eng.*, **4**(1), 43-62. https://doi.org/10.12989/cme.2022.4.1.043.

Han, B., Hui, W.W., Zhang, Q.C., Zhao, Z.Y., Jin, F., Zhang, Q., Lu, T.J. and Lu, B.H. (2018), "A refined quasi-3D zigzag beam theory for free vibration and stability analysis of multilayered composite beams subjected to thermomechanical loading", *Compos. Struct.*, **204**, 620-633. https://doi.org/10.1016/j.compstruct.2018.08.005.

Huang, M.H. and Thambiratnam, D.P. (2001), "Analysis of plate resting on elastic supports and elastic foundation by finite strip method", *Comput. Struct.*, **79**(29-30), 2547-2557. https://doi.org/10.1016/S0045-7949(01)00134-1.

Huang, X., Shan, H., Chu, W. and Chen, Y. (2022), "Computational and mathematical simulation for the size-dependent dynamic behavior of the high-order FG nanotubes, including the porosity under the thermal effects", *Adv. Nano Res.h*, **12**(1), 101-115. https://doi.org/10.12989/anr.2022.12.1.101.

Hussain, M., Asghar, S., Khadimallah, M.A., Ayed, H., Alghamdi, S., Bhutto, J.K., Mahmoud, S.R. and Tounsi, A. (2022), "Effect of dimensionless nonlocal parameter: Vibration of double-walled CNTs", *Comput. Concrete*, **30**(4), 269-276. https://doi.org/10.12989/cac.2022.30.4.269.

Jha, D.K., Kant, T. and Singh, R.K. (2013), "Free vibration response of functionally graded thick plates with shear and normal deformations effects", *Compos. Struct.*, **96**, 799-823.

https://doi.org/10.1016/j.compstruct.2012.09.034.
Kar, V.R. and Panda, S.K. (2015), "Nonlinear flexural vibration of shear deformable functionally graded spherical shell panel", *Steel Compos. Struct.*, **18**(3), 693-709. https://doi.org/10.12989/scs.2015.18.3.693.
Kar,V.R., Mahapatra, T.R. and Panda, S.K. (2015), "Nonlinear flexural analysis of laminated composite flat panel under hygro-thermo-mechanical loading", *Steel Compos. Struct.*, **19**(4), 1011-1033. https://doi.org/10.12989/scs.2015.19.4.1011.
Kharghani, N. and Soares, C.G. (2020), "Experimental, numerical and analytical study of buckling of rectangular composite laminates", *Eur. J. Mech.-A/Solids*, **79**, 103869. https://doi.org/10.1016/j.euromechsol.2019.103869.
Khatir, S., Tiachacht, S., Cuong-Le, T, Quoc Bui, T. and Abdel Wahab, M. (2019), "Damage assessment in composite laminates using ANN-PSO-IGA and Cornwell indicator.", *Compos. Struct.*, **230**, 111509. https://doi.org/10.1016/j.compstruct.2019.111509.
Khatir, S., Tiachacht, S., Cuong-Le, T., Ghandourah, E., Mirjalili, S. and Abdel Wahab, M. (2021), "An improved artificial neural network using arithmetic optimization algorithm for damage assessment in FGM composite plates", *Compos. Struct.*, **273**, 114287. https://doi.org/10.1016/j.compstruct.2021.114.
Kolahchi, R., Safari, M. and Esmailpour, M. (2016), "Dynamic stability analysis of temperature-dependent functionally graded CNT-reinforced visco-plates resting on orthotropic elastomeric medium", *Compos. Struct.*, **150**, 255-265. https://doi.org/10.1016/j.compstruct.2016.05.023.
Kumar, H.S.N. and Kattimani, S. (2022), "Nonlinear analysis of two-directional functionally graded doubly curved panels with porosities", *Struct. Eng. Mech.*, **82**(4), 477-490. https://doi.org/10.12989/sem.2022.82.4.477.
Li, Y.P., She, G.L., Gan, L.L. and Liu, H.B. (2023), "Nonlinear thermal post-buckling analysis of graphene platelets reinforced metal foams plates with initial geometrical imperfection", *Steel Compos. Struct.*, **46**(5), 649-658. https://doi.org/10.12989/scs.2023.46.5.649.
Liu, Y., Wang, X., Liu, L., Wu, B. and Yang, Q. (2022), "On the forced vibration of high-order functionally graded nanotubes under the rotation via intelligent modelling", *Adv. Nano Res.*, **13**(1), 47-61. https://doi.org/10.12989/anr.2022.13.1.047.
Madenci, E. (2019), "A refined functional and mixed formulation to static analyses of fgm beams", *Struct. Eng. Mech.*, **69**(4), 427-437. https://doi.org/10.12989/sem.2019.69.4.427.
Madenci, E. (2021), "Free vibration and static analyses of metal-ceramic FG beams via high-order variational MFEM", *Steel Compos. Struct.*, **39**(5), 493-509. https://doi.org/10.12989/scs.2021.39.5.493.
Madenci, E. and Özütok, A. (2020), "Variational approximate for high order bending analysis of laminated composite plates", *Struct. Eng. Mech.*, **73**(1), 97-108. https://doi.org/10.12989/sem.2020.73.1.097.
Madenci, E. and Özkılıç, Y.O. (2021), "Cyclic response of self-centering SRC walls with frame beams as boundary", *Steel Compos. Struct.*, **40**(2), 157-173. https://doi.org/10.12989/scs.2021.40.2.157.
Madenci, E., Özkılıç, Y.O., Aksoylu, C., Asyraf, M.R.M., Syamsir, A., Supian, A.B.M. and Elizaveta, B. (2023), "Experimental and Analytical investigation of flexural behavior of carbon nanotube reinforced textile based composites", *Materials*., **16**, 2222. https://doi.org/10.3390/ma16062222.
Madenci, E., Özkılıç, Y.O., Aksoylu, C., Asyraf, M.R.M., Syamsir, A., Supian, A.B.M. and Mamaev, N. (2023), "Buckling analysis of CNT-reinforced polymer composite beam using experimental and analytical methods", *Materials.*, **16**, 614. https://doi.org/10.3390/ma16020614.
Man, Y. (2022), "On the dynamic stability of a composite beam via modified high-order theory", *Comput. Concrete*, **30**(2), 151-164. https://doi.org/10.12989/cac.2022.30.2.151.
Mansouri, M.R., Beter, J., Fuchs, P.F., Schrittesser, B. and Pinter, G. (2021), "Quantifying matrix-fiber mechanical interactions in hyperelastic materials", *Int. J. Mech. Sci*., **195**, 106268. https://doi.org/10.1016/j.ijmecsci.2021.106268.
Mantari, J.L. and Canales, F.G. (2016), "A unified quasi-3D HSDT for the bending analysis of laminated beams", *Aerosp. Sci. Technol.*, **54**, 267-275. https://doi.org/10.1016/j.ast.2016.04.026.
Mantari, J.L. and Soares, C.G. (2012), "Generalized hybrid quasi-3D shear deformation theory for the static analysis of advanced composite plates", *Compos. Struct.*, **94**(8), 2561-2575. https://doi.org/10.1016/j.compstruct.2012.02.019.
Mantari, J.L. and Soares, C.G. (2013), "A novel higher-order shear deformation theory with stretching effect for functionally graded plates", *Compos. Part B: Eng.*, **45**(1), 268-281. https://doi.org/10.1016/j.compositesb.2012.05.036.
Matsunaga, H. (2009), "Stress analysis of functionally graded plates subjected to thermal and mechanical loadings", *Compos. Struct.s*, **87**(4), 344-357. https://doi.org/10.1016/j.compstruct.2008.02.002.
Mindlin, R.D. (1951), "Influence of rotatory inertia and shear on flexural motions of isotropic elastic plates", *J. Appl. Mech.*, 31-38. https://doi.org/10.1115/1.4010217.
Mouritz, A.P., Gellert, E., Burchill, P. and Challis, K. (2001), "Review of advanced composite structures for naval ships and submarines", *Compos. Struct.*, **53**(1), 21-42. https://doi.org/10.1016/S0263-8223(00)00175-6.
Mula, S.N., Leite, A.M.S. and Loja, M.A.R. (2022), "Analytical and numerical study of failure in composite plates", *Compos. Mater. Eng.*, **4**(1), 23-41. https://doi.org/10.12989/cme.2022.4.1.023.
Navale, K.U. and Pise, C.P. (2021)., "A review on high order shear deformation theory for orthotropic composite laminates", *Int. J. Eng. Res. Technol.*, **10**(1), 477-481. https://doi.org/10.17577/IJERTV10IS010156.
Neves, A.M.A., Ferreira, A.J.M., Carrera, E., Cinefra, M., Roque, C.M.C., Jorge, R.M.N. and Soares, C.M.M. (2012b), "A quasi-3D hyperbolic shear deformation theory for the static and free vibration analysis of functionally graded plates", *Compos. Struct.*, **94**(5), 1814-1825. https://doi.org/10.1016/j.compstruct.2011.12.005.
Neves, A.M.A., Ferreira, A.J.M., Carrera, E., Cinefra, M., Roque, C.M.C., Jorge, R.M.N. and Soares, C.M. (2013), "Static, free vibration and buckling analysis of isotropic and sandwich functionally graded plates using a quasi-3D higher-order shear deformation theory and a meshless technique", *Compos. Part B: Eng.g*, **44**(1), 657-674. https://doi.org/10.1016/j.compositesb.2012.01.089.
Neves, A.M.A., Ferreira, A.J.M., Carrera, E., Roque, C.M.C., Cinefra, M., Jorge, R.M.N. and Soares, C.M.M. (2012a), "A quasi-3D sinusoidal shear deformation theory for the static and free vibration analysis of functionally graded plates", *Compos. Part B: Eng.*, **43**(2), 711-725. https://doi.org/10.1016/j.compositesb.2011.08.009.
Nikbakt, S., Kamarian, S. and Shakeri, M. (2018), "A review on optimization of composite structures Part I: Laminated composites", *Compos. Struct.*, **195**, 158-185. https://doi.org/10.1016/j.compstruct.2018.03.063.
Noor, A.K. (1973), "Free vibrations of multilayered composite plates", *AIAA J.*, **11**(7), 1038-1039. https://doi.org/10.2514/3.6868.
Onyeka, F.C. and Edozie, O.T. (2021), "Analytical solution of thick rectangular plate with clamped and free support boundary condition using polynomial shear deformation theory", *Adv. Sci. Tech. Eng. Syst. J.*, **6**(1), 1427-1439. https://doi.org/10.25046/aj0601162.

Ozutok, A., Madenci, E. and Kadioglu, F. (2014), "Free vibration analysis of angle-ply laminate composite beams by mixed finite element formulation using the Gâteaux differential", *Sci. Eng. Compos. Mater.*, **21**(2), 257-266. https://doi.org/10.1515/secm-2013-0043.

Pagano, N.J. (1970), "Exact solutions for rectangular bidirectional composites and sandwich plates", *J. Compos. Mater.*, **4**(1), 20-34. https://doi.org/10.1177/002199837000400102.

Polat, A. and Kaya, Y. (2022), "Analysis of discontinuous contact problem in two functionally graded layers resting on a rigid plane by using finite element method", *Comput. Concrete*, **29**(4), 247-253. https://doi.org/10.12989/cac.2022.29.4.247.

Rachedi, M.A., Benyoucef, S., Bouhadra, A., BachirBouiadjra, R., Sekkal, M. and Benachour, A. (2020), "Impact of the homogenization models on the thermoelastic response of FG plates on variable elastic foundation", *Geomech. Eng.*, **22**(1), 65-80. https://doi.org/10.12989/gae.2020.22.1.065.

Ramady, A., Dakhel, B., Balubaid, M. and Mahmoud, S.R. (2020), "A mathematical approach for the effect of the rotation on thermal stresses in the piezo-electric homogeneous material", *Comput. Concrete.*, **25**(5), 471-478. https://doi.org/10.12989/cac.2020.25.5.471.

Ramteke, P.M., Panda, S.K. and Sharma, N. (2019), "Effect of grading pattern and porosity on the eigen characteristics of porous functionally graded structure", *Steel Compos. Struct.*, **33**(6), 865-875. https://doi.org/10.12989/scs.2019.33.6.865.

Reddy, J.N. (2011), "A general nonlinear third-order theory of functionally graded plates", *Int. J. Aerosp. Lightweight Struct.(IJALS)*, **1**(1). https://doi.org/10.3850/S201042861100002X.

Reissner, E. (1944), "On the theory of bending of elastic plates", *J. Math. Phys.*, **23**, 184–191. https://doi.org/10.1002/sapm1944231184.

Reissner, E. (1945), "The effect of transverse shear deformation on the bending of elastic plates", *J. Appl. Mech.*, **12**(2), 69-77. https://doi.org/10.1115/1.4009435.

Rezaiee-Pajand, M., Sobhani, E. and Masoodi, A.R. (2022), "Vibrational behavior of exponentially graded joined conical-conical shells", *Steel Compos. Struct.*, **43**(5), 603-623. https://doi.org/10.12989/scs.2022.43.5.603.

Sayyad, A.S. and Ghugal, Y.M. (2014), "A new shear and normal deformation theory for isotropic, transversely isotropic, laminated composite and sandwich plates", *Int. J. Mech. Mater. Design*, **10**(3), 247-267. https://doi.org/10.1007/s10999-014-9244-3.

Selmi, A. (2020), "Exact solution for nonlinear vibration of clamped-clamped functionally graded buckled beam", *Smart Struct. Syst.*, **26**(3), 361-371. https://doi.org/10.12989/sss.2020.26.3.361.

Selmi, A. (2022), "Dynamic behavior of cracked ceramic reinforced aluminum composite beam", *Smart Struct. Syst.*, **29**(3), 387-393. https://doi.org/10.12989/sss.2022.29.3.387.

Selmi, A. and Bisharat, A. (2018), "Free vibration of functionally graded SWNT reinforced aluminum alloy beam", *J. Vibroeng.*, **20**(5), 2151-2164. https://doi.org/10.21595/jve.2018.19445.

Setoodeh, A.R. and Karami, G. (2004), "Static, free vibration and buckling analysis of anisotropic thick laminated composite plates on distributed and point elastic supports using a 3-D layer-wise FEM", *Eng. Struct.*, **26**(2), 211-220. https://doi.org/10.1016/j.engstruct.2003.09.009.

Shahsavari, D., Karami, B., Fahham, H.R. and Li, L. (2018), "On the shear buckling of porous nanoplates using a new size-dependent quasi-3D shear deformation theory", *Acta Mechanica*, **229**(11), 4549-4573. https://doi.org/10.1007/s00707-018-2247-7.

Shao, D., Wang, Q., Tao, Y., Shao, W. and Wu, W. (2021), "A unified thermal vibration and transient analysis for quasi-3D shear deformation composite laminated beams with general boundary conditions", *Int. J. Mech. Sci.*, **198**, 106357. https://doi.org/10.1016/j.ijmecsci.2021.106357.

She, G.L., Ding, H.X. and Zhang, Y.W. (2022), "Wave propagation in a FG circular plate via the physical neutral surface concept", *Struct. Eng. Mech.*, **82**(2), 225-232. https://doi.org/10.12989/sem.2022.82.2.225.

Sobhy, M. and Zenkour, A.M. (2018), "Nonlocal thermal and mechanical buckling of nonlinear orthotropic viscoelastic nanoplates embedded in a visco-pasternak medium", *Int. J. Appl. Mech.*, **10**(8), 1850086. https://doi.org/10.1142/S1758825118500862.

Soliman A.E., Eltaher M.A., Attia M.A. and Alshorbagy A.E. (2018), "Nonlinear transient analysis of FG pipe subjected to internal pressure and unsteady temperature in a natural gas facility", *Struct. Eng. Mech.*, **66**(1), 85-96. https://doi.org/10.12989/sem.2018.66.1.085.

Talha, M. and Singh, B. (2010), "Static response and free vibration analysis of FGM plates using higher order shear deformation theory", *Appl. Math. Model.*, **34**(12), 3991-4011. https://doi.org/10.1016/j.apm.2010.03.034.

Thai, H.T. and Kim, S.E. (2013), "A simple quasi-3D sinusoidal shear deformation theory for functionally graded plates", *Compos. Struct.*, **99**, 172-180. https://doi.org/10.1016/j.compstruct.2012.11.030.

Tran, T.M. and Cuong-Le, T. (2022), "A nonlocal IGA numerical solution for free vibration and buckling analysis of porous sigmoid functionally graded (P-SFGM) nanoplate", *Int. J. Struct. Stab. Dyn.*, **22**(16), 2250193. https://doi.org/10.1142/S0219455422501930.

Vinyas, M. (2020), "On frequency response of porous functionally graded magneto-electro-elastic circular and annular plates with different electro-magnetic conditions using HSDT", *Compos. Struct.*, **240**, 112044. https://doi.org/10.1016/j.compstruct.2020.112044.

Wang, Y.Q. and Zu, J.W. (2017), " Vibration behaviors of functionally graded rectangular plates with porosities and moving in thermal environment", *Aerosp. Sci. Technol.*, **69**, 550-562. https://doi.org/10.1016/j.ast.2017.07.023.

Wang, Y.Q., Huang, X.B. and Li, J. (2016), "Hydroelastic dynamic analysis of axially moving plates in continuous hot-dip galvanizing process", *Int. J. Mech. Sci.*, **110**, 201-216. https://doi.org/10.1016/j.ijmecsci.2016.03.010.

Wu, X. and Fang, T. (2022), "Intelligent computer modeling of large amplitude behavior of FG inhomogeneous nanotubes", *Adv. Nano Res.*, **12**(6), 617-627. https://doi.org/10.12989/anr.2022.12.6.617.

Xiao, H., Yan, K. and She, G. (2021), "Study on the characteristics of wave propagation in functionally graded porous square plates", *Geomech. Eng.*, **26**(6), 607-615. https://doi.org/10.12989/gae.2021.26.6.607.

Xu, J.Q. and She, G.L. (2022), "Thermal post-buckling analysis of porous functionally graded pipes with initial geometric imperfection", *Geomech. Eng.*, **31**(3), 329-337. https://doi.org/10.12989/gae.2022.31.3.329.

Yaylaci, M. and Avcar, M. (2020), "Finite element modeling of contact between an elastic layer and two elastic quarter planes", *Comput. Concrete.*, **26**(2), 107-114. https://doi.org/10.12989/cac.2020.26.2.107.

Yaylaci, M., Abanoz, M., Yaylacı, E.U., Ölmez, H., Sekban, D.M., and Birinci, A. (2022), "The contact problem of the functionally graded layer resting on rigid foundation pressed via rigid punch", *Steel Compos. Struct.*, **43**(5), 661-672. https://doi.org/10.12989/scs.2022.43.5.661.

Yaylaci, M., Adiyaman, G., Oner, E. and Birinci, A. (2021a), "Investigation of continuous and discontinuous contact cases in the contact mechanics of graded materials using analytical method and FEM", *Comput. Concrete.*, **27**(3), 199-210.

https://doi.org/10.12989/cac.2021.27.3.199.

Yaylaci, M., Yayli, M., Yaylaci, E.U., Olmez, H. and Birinci, A. (2021), "Analyzing the contact problem of a functionally graded layer resting on an elastic half plane with theory of elasticity, finite element method and multilayer perceptron", *Struct. Eng. Mech.*, **78**(5), 585-597. https://doi.org/10.12989/sem.2021.78.5.585.

Ye, L., Lu, Y., Su, Z. and Meng, G. (2005), "Functionalized composite structures for new generation airframes: A review", *Compos. Sci. Technol.*, **65**(9), 1436-1446. https://doi.org/10.1016/j.compscitech.2004.12.015.

Zenkour, A.M. (2007), "Benchmark trigonometric and 3-D elasticity solutions for an exponentially graded thick rectangular plate", *Arch. Appl. Mech.*, **77**(4), 197-214. https://doi.org/10.1007/s00419-006-0084-y.

Zenkour, A.M. (2018), "A quasi-3D refined theory for functionally graded single-layered and sandwich plates with porosities", *Compos. Struct.*, **201**, 38-48. https://doi.org/10.1016/j.compstruct.2018.05.147.

Zenkour, A.M. and El-Shahrany, H.D. (2021), "Quasi-3D theory for the vibration and deflection of a magnetostrictive composite plate resting on a viscoelastic medium", *Compos. Struct*., **269**, 114028. https://doi.org/10.1016/j.compstruct.2021.114028.

Zenzen, R., Khatir, S., Belaidi, I., Cuong-Le, T. and Abdel Wahab, M. (2020), "A modified transmissibility indicator and Artificial Neural Network for damage identification and quantification in laminated composite structures", *Compos. Struct.*, **248**, 112497. https://doi.org/10.1016/j.compstruct.2020.112497.

Zhang W. (2001), "Global and chaotic dynamics for a parametrically excited thin plate", *J Sound Vib.,* **239**, 1013-1036. https://doi.org/10.1006/jsvi.2000.3182.

Zhang, Y.Y., Wang, Y.X., Zhang, X., Shen, H.M. and She, G.L. (2021), "On snap-buckling of FG-CNTR curved nanobeams considering surface effects", *Steel Compos. Struct.*, **38**(3), 293-304. https://doi.org/10.12989/scs.2021.38.3.293.

Zhang, Y.W. and She, G.L. (2022), "Wave propagation and vibration of FG pipes conveying hot fluid", *Steel Compos. Struct.*, **42**(3), 397-405. https://doi.org/10.12989/scs.2022.42.3.397.

Zhang, Y.W., She, G.L. and Ding, H.X. (2023c), "Nonlinear resonance of graphene platelets reinforced metal foams plates under axial motion with geometric imperfections", *Eur. J. Mech. -A/Solids*, **98**, 104887. https://doi.org/10.1016/j.euromechsol.2022.104887.

Zhang, Y.W., Ding, H.X. and She, G.L. (2023a), "Wave propagation in spherical and cylindrical panels reinforced with carbon nanotubes", *Steel Compos. Struct.*, **46**(1), 133-141. https://doi.org/10.12989/scs.2023.46.1.133.

Zhang, Y.W., She, G.L., Gan, L.L. and Li, Y.P. (2023b), "Thermal post-buckling behavior of GPLRMF cylindrical shells with initial geometrical imperfection", *Geomech. Eng.*, **32**(6), 615-625. https://doi.org/10.12989/gae.2023.32.6.615.

Zhang, Y.W. and She, G.L. (2023), "Nonlinear low-velocity impact response of graphene platelet-reinforced metal foam cylindrical shells under axial motion with geometrical imperfection", *Nonlinear. Dyn*., **111**, 6317-6334. https://doi.org/10.1007/s11071-022-08186-9.

Zhou, J., Moradi, Z., Safa, M. and Khadimallah, M.A. (2022), "Intelligent modeling to investigate the stability of a two-dimensional functionally graded porosity-dependent nanobeam", *Comput. Concrete*., **30**(2), 85-97. https://doi.org/10.12989/cac.2022.30.2.085.

Zhu, F.Y., Lim, H.J., Choi, H. and Yun, G.J. (2022), "A hierarchical micromechanics model for nonlinear behavior with damage of SMC composites with wavy fiber", *Compos. Mater. Eng.*, **4**(1), 1-21. https://doi.org/10.12989/cme.2022.4.1.001.